

ALMA MATER STUDIORUM · UNIVERSITY OF BOLOGNA

School of Science
Department of Physics and Astronomy
Master Degree in Physics

**Chiral gravitational waves
from axion-inflation models
with step-like features**

Supervisor:
Dr. Francisco Gil Pedro

Submitted by:
Michael Bacchi

Academic Year 2020/2021

Abstract

Models with an axion-like inflaton have received considerable attention since the early 90's, since pseudo-Nambu Goldstone bosons (pNGBs) have a radiatively stable potential and they are abundant in string theory. In these models, the inflaton can be coupled with a gauge field through the operator $\Phi F_{\mu\nu} \tilde{F}^{\mu\nu}$, leading to a rich phenomenology. The produced gauge quanta source the scalar and tensor components of the metric perturbations, with the latter giving rise to non-vanishing TB and EB correlation functions in the Cosmic Microwave Background (CMB), which can be detected by ongoing and future experiments.

In this work, we study the dynamics of axion-inflation models, both analytically and numerically, focusing mainly on chiral gravitational waves that are generated in three different scenarios: natural inflation, axion monodromy and a linear potential with a step-like feature. We find that a signal can be detected by LISA and by advanced LIGO and Einstein Telescope if the step is broad or very steep, respectively, but in these cases problems related to strong backreaction on Friedmann equation might arise. If instead the step is just a small correction to the linear potential, chiral gravitational waves might be detected by LISA in a weak backreaction regime.

Contents

Abstract	1
Introduction	4
1 The Hot Big Bang theory and its drawbacks	6
1.1 The Standard Cosmological Model	6
1.2 The shortcomings of the standard Big Bang theory	10
2 Slow-roll inflation and cosmological perturbations	13
2.1 Inflation and slow-roll conditions	13
2.2 Cosmological perturbations	16
2.2.1 Scalar cosmological perturbations during inflation	19
2.2.2 Tensor cosmological perturbations during inflation	21
3 Scalar perturbations from axion-inflation models	23
3.1 Introduction to axion-inflation	23
3.2 The slow roll solution	25
3.3 Constraints on the inflaton solution	27
3.4 Scalar perturbations and Power Spectrum	28
3.5 Scalar perturbations in natural inflation	31
3.6 Scalar perturbations in axion monodromy	33
4 Tensor perturbations and Power Spectrum	37
4.1 Generation of tensor modes	37
4.2 Tensor perturbations in natural inflation models	41
4.3 Gravitational waves from axion monodromy inflation	42
4.4 Chiral gravitational waves for a step-like potential	44
5 Conclusions and outlook	53

A	Calculation of the scalar power spectrum	55
A.1	Two-point function of $\delta_{\vec{E}\cdot\vec{B}}$	55
A.2	The Green function	56
A.3	The scalar power spectrum	57
B	Calculation of the tensor power spectrum	59
	Bibliography	62

Introduction

Our Universe is in first approximation homogeneous, isotropic and flat. The Friedmann-Lemaître-Robertson-Walker cosmological model, also known as the Hot Big Bang theory, allows to understand the evolution of the universe so successfully that sensible speculations about the universe at times as early as 10^{-43} sec after the Big Bang are possible. Nevertheless, it is insufficient to account specifically the properties listed above, leading to the flatness problem, the horizon problem and the entropy problem.

Inflation represents a simple and elegant theory that can solve all three of them. In its essence, it represents an early epoch in the history of our Universe when it expanded exponentially. Mathematically, this is translated into aH being an increasing function of time. This condition can be achieved if we consider a quasi-deSitter universe, filled with matter that violates the Strong Energy Condition. In particular, the easiest models which satisfy this requirement, called slow-roll models, consider a scalar field as inflaton with a build-in mechanism to interrupt inflation after a certain amount of time.

In this thesis we will focus in the specific case in which the inflaton is an axion. Axions are the simplest spin-zero particle with a radiatively stable potential, thanks to their broken shift symmetry, and they are also abundant in string theory. In any model of axion inflation, the scalar field is coupled to a gauge field through an interaction of the form $\Phi F_{\mu\nu} \tilde{F}^{\mu\nu}$, where α is the dimensionless coupling constant and f is the axion decay constant. This coupling makes axion inflation phenomenology extremely rich and complex. For instance, the gauge field generates a backreaction effect on both the inflaton dynamics and Friedmann equation, effectively slowing down the axion when it rolls down its potential and extending the duration of inflation. The energy absorbed through this dissipative channel ignites the creation of gauge quanta which become classical and source scalar and tensor perturbations in the metric. In particular, given the parity-violating nature of the system, the tensor modes produced during inflation will also be parity-odd, and they can show up in the CMB in the form of B-modes, the parity-odd, divergence-free component of the polarized radiation. On the other hand, the curl-free component of the CMB, the E-modes, and the temperature anisotropies are parity-even. Therefore, a signal for a non-vanishing $\langle B E \rangle$ or $\langle B T \rangle$ correlation will signal parity violation and might be detected by ongoing and upcoming Earth- and space-based experiments, like

advanced LIGO and LISA. We will verify this hypothesis for three specific axion models: natural inflation, axion monodromy and an ad-hoc model with a suitable modulated linear potential.

This work will be structured as follows. In chapter 1 and 2 we will briefly review the Standard Cosmological Model, its merits and drawbacks, before introducing the concept of inflation and discuss its dynamics. In particular, we will show how scalar and tensor perturbations arise at the cosmological scale in standard slow-roll models. In chapter 3 we will start our treatment of axion inflation by studying the generation of gauge modes at the expenses of the inflaton energy and their conversion into scalar perturbations. The results will be given firstly in full generality and then specifically for the three models we are taking into account. Finally, in chapter 4 we move our attention to the production of gravitational waves and their power spectrum, which can be easily related to the sensitivity curves of current experiments. In particular, we will study the possibility of detecting a chiral signal for all three models.

Chapter 1

The Hot Big Bang theory and its drawbacks

In this first chapter we will review the main features of the Standard Cosmological Model and its drawbacks, which led to the introduction of the concept of inflation. We will briefly show how a period of exponential expansion of the Universe can account all the problems encountered in the Hot Big Bang theory, before introducing the requirements which are essential for all inflation models.

1.1 The Standard Cosmological Model

The Cosmic Microwave Background, also called relic radiation, was first predicted in 1948 by Ralph Alpher and Robert Herman and then experimentally discovered in 1964 by Arno Penzias and Robert Woodrow Wilson. The photons which constitute this radiation are the ones that decoupled from matter in an early stage of the history of our Universe, namely at the last scattering surface. The CMB has a thermal black body spectrum at a temperature of approximately 2.73 K, with anisotropies of at most $\delta T/T \sim 10^{-5}$. Its great degree of homogeneity, together with other astrophysical observations, is the main evidence that supports the *Cosmological Principle*, which states that the Universe looks exactly the same in all directions, i.e. it is homogeneous and isotropic, on sufficiently large scales.

Taking these properties for granted, we can apply it to General Relativity and try to find solutions to Einstein's field equation

$$R_{\mu\nu} - \frac{1}{2}Rg_{\mu\nu} + \Lambda g_{\mu\nu} = 8\pi GT_{\mu\nu}, \quad (1.1)$$

a second-order differential equation for the metric tensor $g_{\mu\nu}$, where $T_{\mu\nu}$ is the energy-momentum tensor of the source we are considering. In general, it is impossible to find

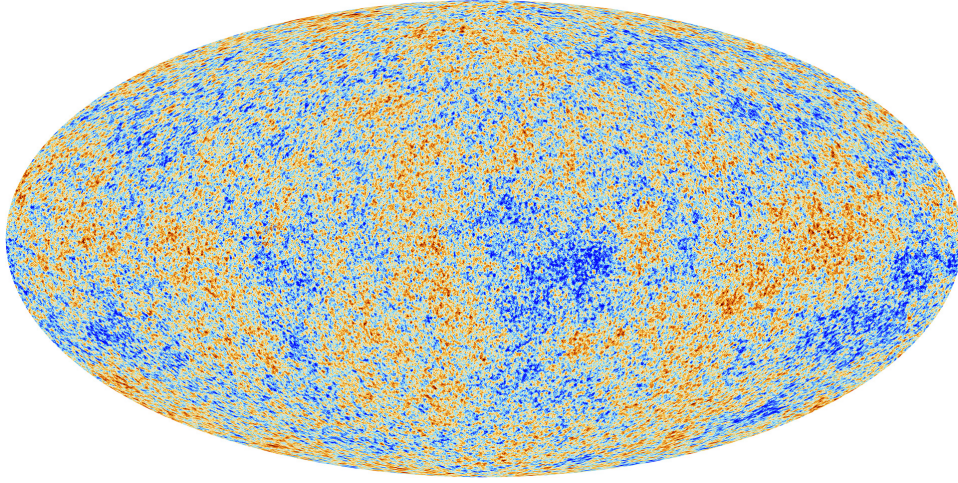


Figure 1.1: The Cosmic Microwave Background as observed by the Planck observatory. The differences in color denote the $\sim 10^{-5}$ energy fluctuations.
Source: https://www.esa.int/ESA_Multimedia/Images/2013/03/Planck_CMB.

analytical solutions to it if there are no symmetries in the system. In our case, homogeneity and isotropy are related to the existence of 3 space-like Killing vectors generating space translations and 3 space-like Killing vectors generating rotations, respectively. Hence, our 4D space-time can be divided into a maximally symmetric three-manifold Ω and a time direction with no related Killing vector, since our Universe is expanding. It can be proven that the Cosmological Principle determines uniquely the *Friedmann-Robertson-Walker* (FRW) metric

$$ds^2 = -dt^2 + a^2(t) \left[\frac{dr^2}{1 - kr^2} + r^2(d\theta^2 + \sin^2(\theta)d\phi^2) \right], \quad (1.2)$$

where t is the proper time of an observer comoving with the cosmic fluid that fills the Universe, a is the scale factor and $k = 0, \pm 1$ is the curvature constant. Depending on the value of k , we have three different cases: a flat space, corresponding to the usual Minkowski space-time, or a closed/open space (de Sitter and Anti de Sitter space), respectively.

In order to solve Einstein equation we need also to define our source. The assumptions of homogeneity and isotropy allow us to consider the Universe filled with a perfect fluid, for which the energy-momentum tensor has the form

$$T_{\mu\nu} = (p + \rho)U_\mu U_\nu - pg_{\mu\nu}, \quad (1.3)$$

where U_μ is the fluid 4-velocity. In the case of a comoving fluid $U_\mu = (-1, \mathbf{0})$, and assuming a flat FRW metric, then the stress-energy tensor becomes $T_{\mu\nu} = \text{diag}(\rho, -p, -p, -p)$.

This tensor must also satisfy the continuity equation $\nabla_\mu T_\nu^\mu = 0$, whose $\nu = 0$ component is

$$\nabla_\mu T_0^\mu = \dot{\rho} + 3H(p + \rho) = 0, \quad (1.4)$$

where the dot implies derivation with respect to the cosmic time t and $H = \dot{a}/a$ is the Hubble parameter. At this point we assume an equation of state for the fluid of the form $p = \omega\rho$, which inserted back in the energy conservation equation gives

$$\frac{\dot{\rho}}{\rho} = -3(1 + \omega)\frac{\dot{a}}{a}, \quad (1.5)$$

whose general solution is

$$\rho(t) \propto a(t)^{-3(1+\omega)}. \quad (1.6)$$

There are some particular cases, depending on the value of ω :

- $\omega = 0$, **dust**. In this case, there is no pressure since the particles do not interact among themselves. The energy density then reads

$$\rho_{\text{dust}}(t) = \frac{E}{V} \propto a(t)^{-3}. \quad (1.7)$$

This result is compatible with the rescaling of the two quantities determining the energy density, namely, the mass of the fluid and its volume. The former is an invariant quantity, while the latter goes like $V \propto a^3$, since every spatial dimension rescales like a .

- $\omega = 1/3$, **radiation**: in this specific scenario, massless particles have no mass scale, so the trace of the energy-momentum tensor has to vanish

$$T_\mu^\mu = T = -\rho + 3p = 0 \rightarrow p = \frac{1}{3}\rho. \quad (1.8)$$

Moreover, the energy density rescales as

$$\rho_{\text{radiation}}(t) \propto a(t)^{-4}, \quad (1.9)$$

as we expect since in addition to the rescale of the volume, also the frequency of the photons redshifts and so rescales as $\nu \propto a^{-1}$.

- $\omega = -1$, **vacuum energy**: Finally, one can also choose an equation of state of the form

$$\rho_\Lambda = -p = \frac{\Lambda}{8\pi G}, \quad (1.10)$$

where Λ is the famous cosmological constant first introduced by Einstein. In this case the energy density does not rescale in time with $a(t)$, and as we will see this property will be fundamental to obtain an accelerated expansion of the Universe.

Now that we have both the FRW metric and the stress-energy tensor of our source which describes our expanding Universe, we can insert both back in Einstein equation. The results are the two *Friedmann equations* for the scale factor $a(t)$:

$$3 \left[\left(\frac{\dot{a}}{a} \right)^2 + \frac{k}{a^2} \right] = 8\pi G \rho, \quad (1.11)$$

$$3 \frac{\ddot{a}}{a} = -4\pi G (\rho + 3p) \quad (1.12)$$

where, technically speaking, the first one is a constraint on the initial conditions of $a(t)$, while its dynamics is described by the second one. It is useful to introduce the density parameter Ω as

$$\Omega := \frac{\rho}{\rho_{\text{critical}}} = \frac{8\pi G}{3H^2} \rho, \quad (1.13)$$

so that the first Friedmann equation becomes

$$\Omega - 1 = \frac{k}{a^2 H^2}. \quad (1.14)$$

In this way we can now classify the topology of our Universe depending on the value of either k , ρ or Ω as follows:

- $\rho < \rho_{\text{critical}}$ or equivalently $\Omega < 1$ or equivalently $k = -1$ corresponds to an open Universe;
- $\rho = \rho_{\text{critical}}$ or equivalently $\Omega = 1$ or equivalently $k = 0$ is a flat Universe;
- $\rho > \rho_{\text{critical}}$ or equivalently $\Omega > 1$ or equivalently $k = +1$ instead represents a closed Universe.

One can also show that once we fix the topology via suitable initial conditions, the Universe evolves in time preserving it. Then, the evolution of the scale factor depends on the value of k and on the specific equation of state of our source. In particular, observations tell us that we are very close to $\Omega = 1$, so our Universe is almost flat, and we can therefore solve Friedmann equations for the three values of ω discussed earlier:

- $\omega = 0$, dust, $\rho \propto a^{-3} \implies \ddot{a} \propto a^{-2} \implies a(t) \propto t^{\frac{2}{3}}$;
- $\omega = 1/3$, radiation, $\rho \propto a^{-4} \implies \ddot{a} \propto a^{-3} \implies a(t) \propto t^{\frac{1}{2}}$;
- $\omega = -1$, vacuum energy, $\rho = \Lambda/(8\pi G) = \text{constant} \implies \ddot{a} = H_0^2 a = (\Lambda/3)a \implies a(t) \propto e^{H_0 t}$, and the Hubble parameter is a constant.

Notice that in the cases of dust and radiation there is always a time $t = 0$ at which the scale factor goes to zero. This represents an unavoidable, physical singularity not related to the choice of the coordinates system, and it is known in the literature as the Big Bang singularity.

1.2 The shortcomings of the standard Big Bang theory

Despite being a very clear and powerful model, the Big Bang theory presents some drawbacks and limits which require the introduction of a new theory, namely inflation. In this section we will briefly introduce the two main problems that arise in the Standard Cosmology model and explain how inflation is able to solve all of them at once.

The flatness problem As we saw earlier, once the initial conditions induce a certain topology, i.e. flat, open or close according to the initial value of the energy density and consequently of k , the Universe evolves maintaining that topology. Whereas an open and close topology lead to an eternal expanding Universe or to a gravitational collapse known as the Big Crunch, respectively, a flat Universe represents a fixed point in which $\Omega = 1$ at all times. Nevertheless, this scenario is unstable, since even a small perturbation will cause a non-zero curvature which will result in an expanding Universe or in the Big Crunch.

Since observations suggest that we live in an almost flat Universe, the condition $\Omega = 1$ had to hold during all the history of the Universe. Today we are living in a vacuum dominated era, and using Friedmann equations we can evolve Ω_0 at present time back to the matter dominated era and then to the radiation dominated period until the Planck time, assuming that Einstein's General Relativity is valid until the Planck era. The final result is

$$|\Omega(t_P) - 1| \sim 10^{-60}. \quad (1.15)$$

Hence, the flatness problem consist precisely in explaining how the initial conditions can be extremely fine-tuned in order to respect the bound on Ω , not a very appealing method.

The horizon problem The second main problem related to the Hot Big Bang theory is the so called horizon problem, which comes directly from the great homogeneity of the CMB. The relic radiation fills all the sky and has a temperature of $T \approx 2.73K$ everywhere we look up to one part per 100000. Therefore, the photons that constitute the CMB should had some time in the past to thermalize with each other. If we consider the comoving particle horizon for a photon propagating in a flat FRW metric and compute the maximum angle in the sky which connects two points that could have been in causal contact during recombination, we find that the all sky can be divided into 10^4 disconnected patches. Hence, the horizon problem arises from the following question: how is it possible that so many casually disconnected regions of the Universe are now at the same temperature $T \approx 2.73K$ within one part per 100000?

One common solution to all the aforementioned problems is to consider a period of accelerated expansion of the Universe, called *inflation*. Indeed, if we introduce a new stage before RD in which $a(t) \propto e^{Ht}$, or equivalently aH is an increasing function of

time with H constant, then the current value of Ω can be easily explained without any fine-tuning once we remember that

$$\Omega - 1 = \frac{k}{a^2 H^2} = \frac{k}{H_0^2} e^{-2H_0 t} \quad (1.16)$$

and therefore by considering two different times at the beginning and at the end of inflation (i.e. at the start of RD), we will have

$$\frac{|\Omega - 1|_{t=t_f}}{|\Omega - 1|_{t=t_I}} = \left(\frac{a_I}{a_f}\right)^2 = e^{-2N}, \quad (1.17)$$

from which we can see that in order to solve the flatness problem is sufficient to have $N \geq 60$, once we require $|\Omega - 1|_{t=t_I}$ to be of order one. Notice that in the last equation we have introduced the *number of efoldings* N as $dN := d \log a$ as time variable.

In addition to this, inflation provides an elegant solution also to the horizon problem. Even if today two points are casually disconnected because the proper distance between them have increased so quickly during inflation, they could have been in causal contact before that epoch in the early Universe. Conversely, the whole observable Universe could be produced by the inflationary process starting from a small homogeneous domain even if the Universe was strongly inhomogeneous outside that domain.

The condition for inflation $d(aH)/dt > 0$ that we have provided can be restated in equivalent forms:

1. $\omega < -1/3$, i.e. a source which violates the strong energy condition (SEC). This can be seen using Friedmann equation:

$$H^2 = \frac{\rho}{3} \implies \dot{a} = \sqrt{\frac{\rho}{3}} a \xrightarrow{d/dt} \ddot{a} = \dot{a} \sqrt{\frac{\rho}{3}} + \frac{a}{2\sqrt{3\rho}} \dot{\rho} \iff \ddot{a} = \frac{\rho a}{6} (-1 - 3\omega), \quad (1.18)$$

so if we have an accelerated expansion $\ddot{a} > 0$ then $\omega < -1/3$;

2. A decreasing comoving horizon, since

$$d_p(t) = \int_0^{t_f} \frac{d\tilde{t}}{a(\tilde{t})} \sim a^{\frac{1}{2}(1+3\omega)}, \quad (1.19)$$

where we have used Friedmann equation and continuity;

3. A slowly decreasing Hubble parameter. From the definition of H , taking its time derivative we have

$$\dot{H} = \frac{\ddot{a}}{a} - \left(\frac{\dot{a}}{a}\right)^2 \implies \frac{\dot{H}}{H^2} = \frac{\ddot{a}a}{\dot{a}^2} - 1 = -\frac{3}{2}(1 + \omega), \quad (1.20)$$

which is negative for $\omega < -1/3$;

4. A source with an energy-momentum tensor which has a negative pressure, as one can see from the equation of state $p = \omega\rho$.

Focusing on the last condition and in the time dependence of a , we see as the only possible source which could develop a stage of inflation is vacuum energy, i.e. a de Sitter space-time. Nevertheless, the field that triggers the exponential expansion of the Universe must have a build-in mechanism to exit inflation and enter the RD era. A de Sitter space-time fails in this particular condition since it is eternal. Moreover it does not contain any other type of matter except the cosmological constant. Nowadays, inflation is described considering sources which realize what is called a quasi-de Sitter space-time. In the following chapter we will review their properties, dynamics and observables.

Chapter 2

Slow-roll inflation and cosmological perturbation

In this chapter we will review in more detail the slow-roll inflation models, their dynamics and properties, as well as show how to treat cosmological perturbations in this setup and how those perturbations can be compared with observations.

2.1 Inflation and slow-roll conditions

As we saw earlier, in order to have inflation it is necessary to have a source with a negative pressure. Within the framework of field theory, the easiest field which can have the correct conditions is a single scalar field ϕ , minimally coupled to gravity. Therefore, the total action of our system will be

$$S = \int d^4x \sqrt{-g} [\mathcal{L}_{EH} + \mathcal{L}(\phi)] = \int d^4x \sqrt{-g} \left[\frac{M_P^2}{2} R + \frac{1}{2} g^{\mu\nu} \partial_\mu \phi \partial_\nu \phi - V(\phi) \right], \quad (2.1)$$

where g is the determinant of the metric tensor $g^{\mu\nu}$, R is the Ricci scalar and $V(\phi)$ is the field potential. By using a perturbative approach, so that the scalar field can be divided into an homogeneous background $\phi(t)$ plus a small perturbation $\delta\phi(t, \vec{x})$, and focusing for the time being on the background in a flat FRW metric, their dynamics are described by Klein-Gordon equation

$$\ddot{\phi} + 3H\dot{\phi} = -V_{,\phi}, \quad (2.2)$$

and Friedmann equation

$$H^2 = \frac{1}{3M_P^2} \left(\frac{\dot{\phi}^2}{2} + V(\phi) \right). \quad (2.3)$$

The energy-momentum tensor of the inflaton $\phi(t)$ can be computed in the standard way as

$$T_{\mu\nu} = \frac{2}{\sqrt{-g}} \frac{\delta S}{\delta g^{\mu\nu}} = \partial_\mu \phi \partial_\nu \phi + g_{\mu\nu} \mathcal{L}, \quad (2.4)$$

and since the background is homogeneous and isotropic by construction, it reduces to the stress-energy tensor of a perfect fluid $T_{\mu\nu} = \text{diag}(\rho, -p, -p, -p)$, where in particular

$$T_{00} = \rho = \frac{\dot{\phi}^2}{2} + V(\phi), \quad (2.5)$$

$$\frac{T^i{}_i}{3} = p = \frac{\dot{\phi}^2}{2} - V(\phi). \quad (2.6)$$

From these expressions we can easily compute the equation of state parameter

$$\omega = \frac{p}{\rho} = \frac{\frac{\dot{\phi}^2}{2} - V(\phi)}{\frac{\dot{\phi}^2}{2} + V(\phi)}, \quad (2.7)$$

from which we can see that in order to satisfy the condition for inflation $\omega \sim -1$, the kinetic term of the inflaton has to be negligible with respect to its potential, i.e. $\dot{\phi}^2 \ll V(\phi)$. This requirement is known as the *slow-roll* condition, since in order to have inflation the scalar field has to slowly roll down its potential. Equivalently, this means that the potential has to be flat and we would therefore expect that also $\ddot{\phi}$ is negligible. Under these requirements, the Klein-Gordon and Friedmann equations can be rewritten as follow

$$3H\dot{\phi} = -V_{,\phi} \quad (2.8)$$

$$H^2 = \frac{1}{3M_P^2} V(\phi), \quad (2.9)$$

which in turn can be used to restate the slow-roll conditions in terms of the inflaton potential:

$$\dot{\phi}^2 \ll V(\phi) \iff \frac{V_{,\phi}}{V} \ll 1 \quad (2.10)$$

$$|\ddot{\phi}| \ll |3H\dot{\phi}| \iff \frac{|V_{,\phi\phi}|}{V} \ll 1. \quad (2.11)$$

Again, these conditions suggest that the inflaton potential should be sufficiently flat in order for the field to slowly roll down on it until it reaches its minimum, when inflation stops since the potential does not dominate anymore.

It is customary to introduce three *Hubble slow-roll parameters*, ϵ , η and κ as follows:

$$\left\{ \begin{array}{l} \epsilon = -\frac{\dot{H}}{H^2}; \end{array} \right. \quad (2.12)$$

$$\left\{ \begin{array}{l} \eta = \frac{d \log \epsilon}{dN} = \frac{\dot{\epsilon}}{H\epsilon}; \end{array} \right. \quad (2.13)$$

$$\left\{ \begin{array}{l} \kappa = \frac{d \log \eta}{dN} = \frac{\dot{\eta}}{H\eta}. \end{array} \right. \quad (2.14)$$

In this way, the slow-roll conditions can be recast as $\epsilon < 1$ and $\eta \ll 1$. It is also possible to write the slow-roll parameters in terms of the scalar potential using the Friedmann equations and the equation of motion for ϕ :

$$\epsilon = \frac{M_P^2}{2} \left(\frac{V_{,\phi}}{V} \right)^2, \quad (2.15)$$

$$\eta = M_P^2 \frac{V_{,\phi\phi}}{V}. \quad (2.16)$$

Despite the constraints given by the slow-roll conditions, one can design several slow-roll models, which are characterised by two independent mass scales: a "height" Λ^4 , corresponding to the vacuum energy density of the field during inflation, and a width μ , which instead represents the change in the field value $\Delta\phi$ during inflation. Those models are usually divided into *small field* and *large field* models, although other possibilities have been studied, like *Hybrid models* or *Plateau models*.

Large field models: In large field models, the inflaton is displaced from the minimum of the potential by an amount usually greater or of order the Planck mass ($\Delta\phi \geq M_P$). They are characterised by $V_{,\phi\phi} > 0$, where the potential is usually polynomial, $V(\phi) = \Lambda^4(\phi/\mu)^p$, or exponential, $V(\phi) = \Lambda^4 \exp(\phi/\mu)$. In this scenarios, slow-roll happens because it is assumed that the Universe emerged from a quantum gravitational state with an energy density comparable to that of the Planck density, resulting in a large friction term in Friedmann equation.

Small field models: The name given to this models comes from the fact that usually the scalar field starts from near an unstable equilibrium taken to be at the origin and slowly rolls down to a stable minimum of its potential, so $\Delta\phi < M_P$. An example of small field models are hill-top models, which are characterised by $V_{,\phi\phi} < 0$, and their potential have the form $V(\phi) = \Lambda^4[1 - (\phi/\mu)^p]$.

2.2 Cosmological perturbations

Since our goal is to compare the theoretical predictions with observations, we need a framework in which we can define observable quantities. We know that the CMB anisotropies are very small, so we will use cosmological perturbations theory to achieve our purposes. Here we will first introduce the theory in full generality, before then specializing it to the specific case of perturbations produced during inflation.

Until now we have studied a scalar field coupled with gravity in a flat FRW metric at the level of the background. Adding small but completely unfixed perturbations to both the metric and the energy-momentum tensor, we have, respectively,

$$g_{\mu\nu}(\tau, \vec{x}) = \bar{g}_{\mu\nu}(\tau) + \delta g_{\mu\nu}(\tau, \vec{x}) \quad (2.17)$$

$$T_{\mu\nu}(\tau, \vec{x}) = \bar{T}_{\mu\nu}(\tau) + \delta T_{\mu\nu}(\tau, \vec{x}). \quad (2.18)$$

Thanks to their smallness, we can study their dynamics by making a perturbative expansion order by order of Einstein equation:

$$O(\delta^0) : \quad \bar{G}_{\mu\nu} = 8\pi G \bar{T}_{\mu\nu} \quad (2.19)$$

$$O(\delta^1) : \quad \delta G_{\mu\nu} = 8\pi G \delta T_{\mu\nu} \quad (2.20)$$

as well as for the continuity equation, which can be written at first order as $\nabla^\mu \delta T_{\mu\nu} = 0$. Then, in order to solve Einstein equation, we have first to develop more explicitly the perturbations for the metric and the stress-energy tensor. Let's start from the latter.

The most general form for each metric component perturbations is given by the following equations:

$$\begin{cases} \delta g_{00} = 2a^2 \Phi, & (2.21) \\ \delta g_{0i} = a^2 (B_{,i} + S_i), & (2.22) \\ \delta g_{ij} = a^2 (2\Psi \delta_{ij} + 2E_{,ij} + F_{i,j} + F_{j,i} + h_{ij}), & (2.23) \end{cases}$$

where Φ, B, Ψ and E are scalar perturbations, S and F are traceless/divergence free vectors and h is a traceless and transverse tensorial perturbation. Moreover, h represents gravitational waves whereas S and F are related to the rotational motion of the fluid, and we will no more take them into account since they are of no interest in primordial cosmology.

In total, they have 10 physical degrees of freedom, but, as one can show by developing the tensorial transformation of the perturbed metric under an infinitesimal coordinate transformation of the form $x^\mu \rightarrow \tilde{x}^\mu = x^\mu + \xi^\mu$, they are not all independent since one has to take into account also gauge invariance. Without dwelling on this matter, we simply say that whereas h is already gauge invariant, for scalar perturbations one can either use

Bardeen's Gauge Invariant Variables

$$\Psi_{\text{GI}} = \Psi + \frac{a'}{a}(B - E') \quad (2.24)$$

$$\Phi_{\text{GI}} = \Phi - \frac{1}{a}[a(B - E')]', \quad (2.25)$$

where the prime denotes derivation with respect to conformal time $\tau = \int dt/a(t)$, or fix the gauge by choosing the *Conformal Newtonian Gauge*, in which $E = B = 0$, as we will assume from now on. In the end, the perturbed metric will be

$$ds^2 = -a^2(1 + 2\Phi)d\tau^2 + a^2[(1 - 2\Psi)\delta_{ij} + h_{ij}]dx^i dx^j. \quad (2.26)$$

Moving to the perturbations of the energy-momentum tensor, we consider, without losing generality, the one for a perfect fluid

$$T^\mu{}_\nu = (\rho + p)U^\mu U_\nu - \delta^\mu{}_\nu p \quad (2.27)$$

and we expand those perturbations as follows

$$\rho = \bar{\rho} + \delta\rho, \quad (2.28)$$

$$p = \bar{p} + \delta p, \quad (2.29)$$

$$U^\mu = \bar{U}^\mu + \delta U^\mu, \quad (2.30)$$

where the four-velocity is time-like and normalized as usual $U^\mu U_\mu = 1$. Manipulating the four-velocity, one finds that

$$U^0 = \frac{1}{a}(1 + \delta U^0), \quad (2.31)$$

$$U^i = \frac{1}{a}\delta v^i, \quad (2.32)$$

with $\delta U^0 = -h_{00}/2$. Hence, it is possible to find first the expression for U_0 and finally the expression for $\delta T^\mu{}_\nu$:

$$\left\{ \begin{array}{l} \delta T^0{}_0 = \delta\rho, \end{array} \right. \quad (2.33)$$

$$\left\{ \begin{array}{l} \delta T^0{}_i = -v_i(r\bar{h}_0 + \bar{p}), \end{array} \right. \quad (2.34)$$

$$\left\{ \begin{array}{l} \delta T^i{}_j = -\delta^i{}_j \delta p. \end{array} \right. \quad (2.35)$$

From the continuity equation instead one has two constraints:

$$\left\{ \begin{array}{l} \delta\rho' + 3\frac{a'}{a}(\delta\rho + \delta p) + (\bar{\rho} + \bar{p})(\partial_i v_i - \frac{1}{2}h_{ii}^2) = 0 \quad \nu = 0 \end{array} \right. \quad (2.36)$$

$$\left\{ \begin{array}{l} \partial_i \delta p + (\bar{\rho} + \bar{p})(4\frac{a'}{a}v_i + \frac{1}{2}\partial_i h_{00}) + [v_i(\bar{p} + \bar{\rho})'] = 0 \quad \nu = i. \end{array} \right. \quad (2.37)$$

At this point we have all the information that we need to solve Einstein's equation, which in the specific case of a single, perfect fluid (i.e. in absence of anisotropic stress) appears as

$$\left\{ \begin{aligned} \delta G^0_0 &= \frac{2}{a^2} \left(-\partial^i \partial_i \Psi + 3 \frac{a'}{a} \Psi' - 3 \left(\frac{a'}{a} \right)^2 \Phi \right) = 8\pi G \delta T^0_0 = 8\pi G \delta \rho, \end{aligned} \right. \quad (2.38)$$

$$\left\{ \begin{aligned} \delta G^0_i &= \frac{2}{a^2} \left(-\partial_i \Psi' + \frac{a'}{a} \partial_i \Phi \right) = 8\pi G (\bar{\rho} + \bar{p}) \partial_i v, \end{aligned} \right. \quad (2.39)$$

$$\left\{ \begin{aligned} \delta G^i_j &= \frac{1}{a^2} \partial^i \partial_j (\Phi + \Psi) - \frac{2}{a^2} \delta^i_j \left[-\psi'' + \frac{1}{2} \partial^k \partial_k (\Phi + \Psi) + \frac{a'}{a} (\Phi' - 2\Psi') + \right. \\ &\quad \left. + 2 \frac{a''}{a} \Phi - \left(\frac{a'}{a} \right)^2 \Phi \right] = -8\pi G \delta^i_j \delta p. \end{aligned} \right. \quad (2.40)$$

These equations, together with the constraints on T^μ_ν in equations (2.36) and (2.37), can be simplified by noticing that equation (2.41) reduces to $\partial^i \partial_j (\Phi + \Psi) = 0 \iff \Phi = \Psi$ when $i \neq j$.

In the end, these five equations can be used to obtain a *master equation* for Φ

$$\Phi'' + 3 \frac{a'}{a} \Phi' (1 + c_s^2) - c_s^2 \partial^i \partial_i \Phi + \left[2 \frac{a''}{a} - \left(\frac{a'}{a} \right)^2 (1 - 3c_s^2) \right] \Phi = 4\pi G a^2 (\delta p - c_s^2 \delta \rho), \quad (2.41)$$

where c_s , defined by $\delta p = c_s^2 \delta \rho$, is the speed of sound for the fluid perturbations in the case there is no entropy perturbations. Moreover, since the fluid is perfect, one has that $c_s^2 = \omega$ everywhere in the evolution of the Universe, except for the transitions between radiation/matter and matter/vacuum. Under this further assumption and using Friedmann equations, the master equation assume the final form

$$\Phi'' + 3 \frac{a'}{a} (1 + c_s^2) \Phi' - c_s^2 \partial^i \partial_i \Phi = 0. \quad (2.42)$$

Instead of solving it for some specific cases, like for example non-relativistic or ultra-relativistic matter, we will proceed directly to develop the same machinery in the case the perturbations are produced during inflation.

and knowing that

$$\frac{z''}{z} = \frac{\nu^2 - 1/4}{\tau^2}, \quad (2.53)$$

where $\nu \simeq 3/2 + \epsilon + \eta/2$, Mukhanov-Sasaki equation becomes

$$u_{\mathbf{k}}'' + \left(k^2 - \frac{\nu^2 - 1/4}{\tau^2} \right) u_{\mathbf{k}} = 0. \quad (2.54)$$

Its solution can be given in terms of Hankel functions

$$u_{\mathbf{k}}(\tau) = \sqrt{\tau} [C_1 H_\nu^{(1)}(-k\tau) + C_2 H_\nu^{(2)}(-k\tau)] \quad (2.55)$$

where the constants C_1 and C_2 are fixed once we choose a vacuum. In our case we will impose that the modes reduce to the usual Minkowski ones $u_{\mathbf{k}} = 1/(\sqrt{2k})e^{ik\tau}$ in the far past, i.e. for $|k\tau| \gg 1$, which means $C_1 = 0$ and $C_2 = \sqrt{\pi}/2$. Hence, the solution to Mukhanov-Sasaki equation is given by the so called *Bunch-Davis modes*:

$$u_{\mathbf{k}}(\tau) = \frac{\sqrt{\pi}}{2} \sqrt{-\tau} H_\nu^{(2)}(-k\tau). \quad (2.56)$$

In order to compare our theoretical predictions with experimental results, the main observable used in the literature is the so called scalar power spectrum. It is defined as

$$\langle 0 | \hat{u}_{\mathbf{k}}, \hat{u}_{\mathbf{k}'} | 0 \rangle = |u_{\mathbf{k}}|^2 \delta^{(3)}(\mathbf{k} + \mathbf{k}') = P_u(k) \delta^{(3)}(\mathbf{k} + \mathbf{k}'), \quad (2.57)$$

together with its dimensionless version

$$\mathcal{P}_u(k) := \frac{k^3}{2\pi^2} P_u(k). \quad (2.58)$$

Equivalently, one can define the power spectrum for the *comoving curvature perturbations* $\zeta = u/z$ by simply dividing the expressions above by z^2 , obtaining:

$$\mathcal{P}_\zeta(k) = \frac{k^3}{2\pi^2} \left| \frac{u_{\mathbf{k}}}{z} \right|^2. \quad (2.59)$$

An explicit calculation in the case of a quasi de Sitter spacetime for super-horizon scales gives as a result

$$\begin{aligned} P_\zeta(k \ll aH) &= \frac{1}{z^2} P_u(k \ll aH) = \frac{2^{2\nu-3}}{\pi \epsilon a^2 k} \left(\frac{k}{aH} \right)^{1-2\nu} \Gamma^2(\nu) \implies \\ \mathcal{P}_\zeta(k) &= \frac{H^2}{8\pi^2 \epsilon} \left(\frac{k}{aH} \right)^{3-2\nu} = \mathcal{A}_s \left(\frac{k}{k*} \right)^{n_s-1}, \end{aligned} \quad (2.60)$$

where \mathcal{A}_s is the amplitude of the scalar perturbations, $\nu = 3/2 + \epsilon + \eta/2$, $n_s = 1 - 2\epsilon - \eta$ is the spectral index and $k*$ is the pivot scale. Both \mathcal{A}_s and n_s , together with the dimensionless scalar power spectrum, are tied by observational constraints [24], which are

$$\mathcal{P}_\zeta(k_{\text{CMB}}) = 2.5 \cdot 10^{-9}, \quad (2.61)$$

$$n_s = 0.9649 \pm 0.0042 \quad (\text{at } 68\% \text{ CL}). \quad (2.62)$$

2.2.2 Tensor cosmological perturbations during inflation

Proceeding in a similar way as we did for the scalar case, we will now work out the tensor power spectrum. Again, the starting point are the tensorial part of the perturbed metric

$$ds^2 = -a(\tau)^2 d\tau^2 + a(\tau)^2 (\delta_{ij} + h_{ij}) dx^i dx^j, \quad (2.63)$$

and the perturbed stress-energy tensor. One can show that only the ij component of Einstein tensor is different from zero

$$\delta G_j^i = \frac{1}{a^2} \left(h_{ij}'' + 2 \frac{a'}{a} h_{ij}' - \partial^l \partial_l h_{ij} \right), \quad (2.64)$$

but since $T_j^i \propto \delta_j^i$, then the corresponding Einstein equation has no source on the right-hand side. In the end, Einstein equation reads

$$\left(h_{ij}'' + 2 \frac{a'}{a} h_{ij}' - \partial^l \partial_l h_{ij} \right) = 0. \quad (2.65)$$

Physically, this means that a perfect fluid with no anisotropic stress can not produce gravitational waves.

Moving to Fourier space, we express

$$h_{ij}(\tau, \mathbf{x}) = \frac{1}{(2\pi)^3/2} \int_{\mathbb{R}^3} d^3k \left[h_{\mathbf{k}}^{(+)}(\tau) e_{ij}^{(+)}(\mathbf{k}) + h_{\mathbf{k}}^{(\times)}(\tau) e_{ij}^{(\times)}(\mathbf{k}) \right] e^{i\mathbf{k}\cdot\mathbf{x}} \quad (2.66)$$

in terms of the polarizations tensors for the $+$ and the \times modes, $e_{ij}^{+\times}(\mathbf{k})$, and we solve eq. (2.66) as we previously did. We introduce a new variable $v_{\mathbf{k}}^{(\cdot)} = ah_{\mathbf{k}}^{(\cdot)}/2$, where (\cdot) denotes either $(+)$ or (\times) , such that the equation of motion becomes

$$v_{\mathbf{k}}^{(\cdot)''} + \left(k^2 - \frac{a''}{a} \right) v_{\mathbf{k}}^{(\cdot)} = 0, \quad (2.67)$$

specular to the one for the scalar perturbations except for the effective mass term, which has a''/a instead of z''/z . Thanks to this similarity, its solution is again given in terms of Hankel functions, and imposing Bunch-Davis initial conditions we have

$$v_{\mathbf{k}}^{(\cdot)}(\tau) = \frac{\sqrt{-\pi\tau}}{2} H_{\nu_T}^{(2)}(-k\tau), \quad (2.68)$$

where now $\nu_T = 3/2 + \epsilon$.

Analogous definitions can be made for the tensor power spectrum and its dimensionless variant. For super-horizon scales, the latter has the form

$$\mathcal{P}_h(k \ll aH) = \frac{2H^2}{\pi^2} \left(\frac{k}{aH} \right)^{3-2\nu_T} = \mathcal{A}_t \left(\frac{k}{aH} \right)^{3-2\nu_T}, \quad (2.69)$$

so in this case $n_T = 3 - 2\nu_t = -2\epsilon$.

Finally, we define the tensor-to-scalar ratio r as

$$r := \frac{\mathcal{A}_T}{\mathcal{A}_s} = 16\epsilon, \tag{2.70}$$

which is bounded by experiment to be $r < 0.056$ at 95% CL [26].

Chapter 3

Scalar perturbations from axion-inflation models

In this chapter, we will start our description of axion-inflation models. In particular, we will focus on the dynamics of the system and the generation of scalar perturbations, with the final result represented by the power spectrum of those perturbations. In the first 4 sections the subject will be treated in full generality, i.e. without specifying the form of the inflaton potential, whereas the last 2 parts of this chapter will apply the results to two specific models, namely natural inflation and axion monodromy.

3.1 Introduction to axion-inflation

Even in its simplicity, a compelling particle physics realization of inflation is still lacking. The main obstruction comes from the requirement to have a sufficiently flat scalar potential, with slow-roll parameters $\epsilon, \eta \ll 1$. These parameters are extremely sensitive to UV corrections, leading to fine-tuning problems that have to be addressed in any particle physics model of inflation.

Luckily, Pseudo-Nambu-Goldstone-Bosons (PNGB) represent excellent inflation candidates in an UV complete theory that includes also gravity. Indeed, axion-like particles are the simplest spin-zero degrees of freedom, with a shift symmetry $\varphi \rightarrow \varphi + \text{const}$ broken either explicitly or by quantum effects which provides a radiatively stable potential. Moreover, axions are plentiful in string theory compactifications.

In any axion inflation model, the inflaton is minimally coupled to gravity and is also expected to couple with some gauge field A_μ via interactions of the type

$$\mathcal{L}_{\text{int}} = -\frac{\alpha}{4f}\Phi F^{\mu\nu}\tilde{F}_{\mu\nu}, \quad (3.1)$$

where $F_{\mu\nu} = \partial_\mu A_\nu - \partial_\nu A_\mu$ is the field strength and $\tilde{F}^{\mu\nu} = \frac{1}{2}\varepsilon^{\mu\nu\alpha\beta}F_{\alpha\beta}$ is its dual. As one can see, the strength of the interaction is controlled by the axion decay constant f and the dimensionless parameter α . Through this coupling the kinetic energy of the rolling inflaton is partially transferred into gauge field fluctuations, which in turn produce inflaton fluctuations via either a back-reaction effect or via an inverse decay process of the form $\delta A + \delta A \rightarrow \delta\Phi$, as we will discuss later on in this chapter. Taking into account also this contribution, the total Lagrangian density has the form

$$\mathcal{L} = -\left[\frac{1}{2}(\partial\Phi)^2 + V(\Phi) + \frac{1}{4}F_{\mu\nu}F^{\mu\nu} + \frac{\alpha}{4f}\Phi F_{\mu\nu}\tilde{F}^{\mu\nu}\right] \quad (3.2)$$

where for the time being we will keep the potential $V(\Phi)$ arbitrary and $f \lesssim M_P$. The equations of motion can be found using Maxwell's and Klein-Gordon's equations. In terms of the electric and magnetic fields \vec{E} and \vec{B} and as a function of conformal time τ , they have the following form

$$\begin{aligned} \Phi'' + 2aH\Phi' - \nabla^2\Phi + a^2\frac{dV(\Phi)}{d\Phi} &= \frac{\alpha}{f}a^2\vec{E} \cdot \vec{B}, \\ \vec{E}' + 2aH\vec{E} - \nabla \times \vec{B} &= -\frac{\alpha}{f}\Phi'\vec{B} - \frac{\alpha}{f}\vec{\nabla}\Phi \times \vec{E}, \\ \vec{\nabla} \cdot \vec{E} &= -\frac{\alpha}{f}(\vec{\nabla}\Phi) \cdot \vec{B}, \end{aligned} \quad (3.3)$$

where $H \equiv a'(\tau)/a^2(\tau)$ and where the prime denotes differentiation with respect to conformal time τ . The Bianchi identities are $\vec{B}' + 2aH\vec{B} + \vec{\nabla} \times \vec{E} = 0$ and $\vec{\nabla} \cdot \vec{B} = 0$. The other fundamental equation we will use throughout the following chapters is Friedmann equation, which in cosmological time reads

$$3M_P^2 H^2 = \frac{1}{2}\dot{\Phi}^2 + V(\Phi) + \frac{1}{2}(\vec{E}^2 + \vec{B}^2). \quad (3.4)$$

Notice by inspecting the first equation in (3.3) and in the one above that the fluctuations in the gauge field can have two types of back-reaction: they give rise to a dissipative term into the homogeneous Klein-Gordon equation and they enter as a new source into Friedmann equation through their energy density. In what follows, we will still consider the back-reaction of the gauge field on the inflaton, while we will neglect it in the second case.

3.2 The slow roll solution

Since the inflaton is homogeneous, we have that $\vec{\nabla}\Phi = 0$, and we can introduce the vector potential $\vec{A}(\tau, \vec{x})$ such that $a^2\vec{B} = \vec{\nabla} \times \vec{A}$ and $a^2\vec{E} = -\vec{A}'$. The equations for \vec{A} then read

$$\left(\frac{\partial^2}{\partial \tau^2} - \nabla^2 - \alpha \frac{\Phi'}{f} \vec{\nabla} \times \right) \vec{A} = 0, \quad \vec{\nabla} \cdot \vec{A} = 0. \quad (3.5)$$

At this point, we promote \vec{A} to an operator $\vec{\hat{A}}(\tau, \vec{x})$ and decompose it into annihilation and creation operators

$$\vec{\hat{A}} = \sum_{\lambda=\pm} \int \frac{d^3k}{(2\pi)^{3/2}} \left[\vec{\epsilon}_\lambda(\vec{k}) A_\lambda(\tau, \vec{k}) a_{\lambda\vec{k}} e^{i\vec{k}\cdot\vec{x}} + h.c. \right], \quad (3.6)$$

where the helicity vectors $\vec{\epsilon}_\pm$ have the properties $\vec{k} \cdot \vec{\epsilon}_\pm = 0$, $\vec{k} \times \vec{\epsilon}_\pm = \mp i|\vec{k}|\vec{\epsilon}_\pm$. Then, the equations of motion for \vec{A} are translated in the following equations for A_\pm

$$A_\pm'' + (k^2 \mp \alpha k \frac{\Phi'}{f}) A_\pm = 0. \quad (3.7)$$

Since we are interested in inflationary solutions, we assume that $a(\tau) \simeq -1/(H\tau)$ and $d\Phi/dt \equiv \dot{\Phi}_0 = \text{constant}$. Hence, the equation for A_\pm reduces to

$$\frac{d^2 A_\pm(\tau, k)}{d\tau^2} + \left[k^2 \pm 2k \frac{\xi}{\tau} \right] A_\pm(\tau, k) = 0, \quad (3.8)$$

where we have defined the quantity

$$\xi \equiv \alpha \frac{\dot{\Phi}_0}{2fH}. \quad (3.9)$$

One of the two solutions between A_+ and A_- will develop an instability, depending on the sign of ξ . Without losing generality, we assume that $\alpha > 0$ and $\dot{\Phi} > 0$, so that overall $\xi > 0$.

Looking for solutions which have positive frequency in the sub-horizon regime, when $|\vec{k}|\tau \rightarrow -\infty$, we have that

$$A_\pm(\tau, k) = \frac{1}{\sqrt{2k}} [iF_0(\pm\xi, -k\tau) + G_0(\pm\xi, -k\tau)], \quad (3.10)$$

where F_0 and G_0 are the regular and irregular Coulomb wave functions, respectively. When the second term in brackets in (3.8) dominates over the first one, i.e. when $|k\tau| \ll 2\xi$, one can see by inspecting the limiting form of those functions that A_+ gets rapidly amplified, since it is well approximated by

$$A_+(\tau, k) \simeq \frac{1}{\sqrt{2k}} \left(\frac{k}{2\xi aH} \right)^{1/4} e^{\pi\xi - 2\sqrt{2\xi k/aH}}. \quad (3.11)$$

On the other hand, the modes A_- are not amplified by a factor $e^{\pi\xi}$ by the rolling inflaton, so from now on we will ignore them.

We can now find the slow roll solution for the pseudoscalar inflaton Φ , including the contribution from the backreaction of the gauge field on Φ . Using the decomposition of \vec{A} described above, the right hand side of equation (3.3) can be rewritten as

$$\langle \vec{E} \cdot \vec{B} \rangle = -\frac{1}{a^4} \int \frac{d^3k}{(2\pi)^3} \frac{|\vec{k}|}{2} \frac{\partial}{\partial\tau} (|A_+|^2 - |A_-|^2), \quad (3.12)$$

that can be simplified by using the approximation for A_+ in equation (3.11) and setting $A_- \simeq 0$. Indeed, we notice that the integral above is dominated by small momentum modes with $(8\xi)^{-1} \lesssim k_c/Ha(\tau) \lesssim 2\xi$, and rapidly decreases outside that region. We therefore extend the integration interval from 0 to $+\infty$, and we approximate $dA_+/d\tau \simeq \sqrt{2\xi k a H} A_+$, so that in the end the gauge field term reduces to

$$\langle \vec{E} \cdot \vec{B} \rangle \simeq -\left(\frac{H}{\xi}\right)^4 e^{2\pi\xi} \times \left[\frac{1}{2^{21}\pi^2} \int_0^\infty dx x^7 e^{-x} \right]. \quad (3.13)$$

The term in square brackets can be computed numerically, giving

$$\mathcal{I} \equiv \frac{7!}{(2^{21}\pi^2)} \simeq 2.4 \times 10^{-4}. \quad (3.14)$$

Plugging back in equation (3.3) the result for $\langle \vec{E} \cdot \vec{B} \rangle$, Klein-Gordon equation for the inflaton now reads, in physical time,

$$\frac{d^2\Phi}{dt^2} + 3H \frac{d\Phi}{dt} + V'(\Phi) = -\frac{\mathcal{I}\alpha}{f} \left(\frac{H}{\xi}\right)^4 e^{2\pi\xi}. \quad (3.15)$$

In this section, our goal is to find inflationary solutions where slow roll is supported by the dissipation into electromagnetic modes. So, we assume that both $\ddot{\Phi}$ and $3H\dot{\Phi}$ are negligible with respect to $V'(\Phi)$. In this way, an approximate solution of equation (3.15) is

$$\xi \simeq \frac{1}{2\pi} \log \left[\frac{9}{\mathcal{I}\alpha} \frac{M_P^4 f |V'(\Phi)|}{V^2(\Phi)} \right], \quad (3.16)$$

where we have assumed that $3M_P^2 H^2 = \frac{1}{2}\dot{\Phi}^2 + V(\Phi) + \frac{1}{2}(\vec{E}^2 + \vec{B}^2) \simeq V(\Phi)$.

3.3 Constraints on the inflaton solution

The approximate solution for the quantity ξ have been found under different requirements, from which we can derive several constraints:

- i. First of all, we want to approximate $H^2 \simeq V(\Phi)/3M_P^2$, as in standard slow roll inflation. This requires that both $\langle \vec{E}^2 + \vec{B}^2 \rangle$ and $\dot{\Phi}^2$ be negligible with respect to $V(\Phi)$. With similar techniques to the ones we used for computing $\langle \vec{E} \cdot \vec{B} \rangle$, we can estimate

$$\frac{1}{2}\langle \vec{E}^2 + \vec{B}^2 \rangle = \frac{6! e^{2\pi\xi} H^4}{2^{19}\pi^2 \xi^3} \simeq \frac{4}{7} \frac{\xi}{\alpha} f V'(\Phi), \quad (3.17)$$

where we have used the relation $\mathcal{I}\alpha(H/\xi)^4 e^{2\pi\xi} \simeq f|V'(\Phi)|$. These conditions are satisfied for $\alpha \gg \xi$, for which the energy in the electromagnetic field can be neglected with respect to the energy in the inflaton, unless we are close to the minimum of the potential.

Moving to the second condition $\dot{\Phi}^2/2 \ll V$, by using $\dot{\Phi} = 2fH\xi/\alpha$, we obtain

$$\frac{\dot{\Phi}^2}{2V(\Phi)} = 2 \frac{\xi^2 f^2 H^2}{\alpha^2 V(\Phi)} \simeq \frac{2}{3} \frac{\xi^2}{\alpha^2} \frac{F^2}{M_P^2}. \quad (3.18)$$

This result shows that the kinetic energy of the inflaton can be neglected with respect to the potential energy for $(\xi/\alpha)(f/M_P) \ll 1$, which is equivalent again to the condition $\alpha \gg \xi$, since $f \lesssim M_P$;

- ii. One has also to check whether this solution actually corresponds to an inflating Universe. To do it, we compute the slow roll parameter

$$\epsilon \equiv -\dot{H}/H^2 = \frac{1}{2M_P^2 H^2} \left[\dot{\Phi}^2 + \frac{2}{3} \langle \vec{E}^2 + \vec{B}^2 \rangle + \frac{\vec{\nabla} \cdot (\vec{E} \times \vec{B})}{3aH} \right], \quad (3.19)$$

where we have used the equations of motion and $\langle \vec{\nabla} \cdot (\vec{E} \times \vec{B}) \rangle$. By inserting into equation (3.19) the expressions for $\dot{\Phi}^2$, $\langle \vec{E}^2 + \vec{B}^2 \rangle$ and H^2 found above, we finally derive the result

$$\epsilon \simeq \frac{2\xi^2}{\alpha^2} \frac{f^2}{M_P^2} + \frac{8}{7} \frac{\xi}{\alpha} \frac{f V'(\Phi)}{V(\Phi)}. \quad (3.20)$$

Hence, the condition for inflation $\epsilon < 1$ is satisfied as long as the constraint in *i* is satisfied;

iii. Next we have to find out for which values of the parameters the terms $\ddot{\Phi}$ and $3H\dot{\Phi}$ can be neglected. The conditions to satisfy are the following:

(a)

$$\frac{3H\dot{\Phi}}{V'} \sim \frac{\xi}{2\alpha} \frac{fV/V'}{M_P^2} \ll 1, \quad (3.21)$$

(b)

$$\frac{\ddot{\Phi}}{V'} \sim \frac{2\xi}{3\alpha} \left(-\epsilon \frac{fV/V'}{M_P^2} + \frac{f^2}{\pi M_P^2} \frac{VV''/V'^2 - 2}{\alpha} \right) \ll 1. \quad (3.22)$$

Again, since $fV/V' = \mathcal{O}(f^2)$ and $VV''/V'^2 = \mathcal{O}(1)$, unless we are close to the minimum of the potential, then $\alpha \gg \xi \gtrsim 1$ guarantees that both (a) and (b) hold;

iv. Finally, the last and strongest constraint comes from the requirement that inflation lasts for long enough. To check it, we compute the number of efoldings, given by

$$N \simeq \int_{\Phi_i}^{\Phi_f} \frac{H d\Phi}{\dot{\Phi}} = \frac{\alpha}{2f} \int_{\Phi_i}^{\Phi_f} \frac{d\Phi}{\xi} \simeq \frac{\alpha}{2\xi} \frac{\Phi_f - \Phi_i}{f}. \quad (3.23)$$

Since we have that $|\Phi_f - \Phi_i| \lesssim \pi f$, the above equation implies that $\alpha \gtrsim 2\xi N/\pi$.

3.4 Scalar perturbations and Power Spectrum

Now that we have obtained the slow roll solutions for both the inflaton Φ and the gauge field \vec{A} and the corresponding constraints that apply to the case, we can look for their perturbations and power spectrum.

In our setup, perturbations in Φ arise from the classical inhomogeneities in the electromagnetic field, whereas usually they are generated by quantum fluctuations of the inflaton which are amplified by the evolving background. To begin with, we define ζ to be the curvature perturbation on a uniform energy density hypersurface. This quantity equals the perturbation of the number of efoldings $\zeta = \delta N \equiv N(x) - \bar{N}$, where \bar{N} is the number of efoldings in case of an homogeneous background. If we write the perturbed value of the axion as $\Phi = \Phi_0 + \phi(\tau, \vec{x})$, then $\zeta = H\phi/\dot{\Phi}_0$. Hence, if we want to compute the power spectrum for ζ , we have to first compute the two-point function of ϕ .

The inflaton perturbation ϕ obeys the equation

$$\phi'' + 2aH\phi' + (-\nabla^2 + a^2V'')\phi = -\frac{\alpha}{f} a^2 \delta[\vec{E} \cdot \vec{B}], \quad (3.24)$$

where the fluctuation $\delta[\vec{E} \cdot \vec{B}](\tau, \vec{x})$ gets two main contributions: the intrinsic inhomogeneities in $\vec{E} \cdot \vec{B}$, which would be present even if $\phi = 0$, and a further one that comes

from the fact that $\langle \vec{E} \cdot \vec{B} \rangle$ depends on $\dot{\Phi}$. As a consequence, when we substitute $\Phi + \phi$ to Φ , then $\langle \vec{E} \cdot \vec{B} \rangle$ will become

$$\langle \vec{E} \cdot \vec{B} \rangle + \dot{\phi} \frac{\partial \langle \vec{E} \cdot \vec{B} \rangle}{\partial \dot{\Phi}}. \quad (3.25)$$

Therefore, the fluctuation in equation (3.24) can be expressed in the following way

$$\delta[\vec{E} \cdot \vec{B}] \simeq [\vec{E} \cdot \vec{B} - \langle \vec{E} \cdot \vec{B} \rangle]_{\phi=0} + \frac{\partial \langle \vec{E} \cdot \vec{B} \rangle}{\partial \dot{\Phi}} \dot{\phi}. \quad (3.26)$$

In the second term of the right hand side, $\langle \vec{E} \cdot \vec{B} \rangle$ depends on $\dot{\Phi}$ only through ξ . Since $\partial \langle \vec{E} \cdot \vec{B} \rangle / \partial \xi \simeq 2\pi \langle \vec{E} \cdot \vec{B} \rangle$, using the background equation $\alpha \langle \vec{E} \cdot \vec{B} \rangle / f \simeq V'$ we can rewrite it as $\pi \alpha V' \dot{\phi} / (fH)$. Instead, we will denote the term in square brackets by $\delta_{\vec{E} \cdot \vec{B}}(\tau, \vec{x})$. Moving to Fourier space, the equation of motion for the perturbation ϕ will be

$$\phi''(\vec{p}) - \frac{2}{\tau} \left(1 - \frac{\pi \alpha V'}{2fH^2} \right) \phi'(\vec{p}) + \left(p^2 + \frac{V''}{H^2 \tau^2} \right) \phi(\vec{p}) = -\frac{\alpha}{f} a^2 \int \frac{d^3x}{(2\pi)^{3/2}} e^{-i\vec{p}\vec{x}} \delta_{\vec{E} \cdot \vec{B}}(\tau, \vec{x}). \quad (3.27)$$

Once we denote with $G(\tau, \tau')$ the Green function associated to the differential operator acting on ϕ in the equation above, the correlator of the inflaton in momentum space reads

$$\langle \phi(\vec{p}) \phi(\vec{p}') \rangle = \frac{\alpha^2}{f^2} \int d\tau' d\tau'' G(\tau, \tau') G(\tau, \tau'') a'^2 a''^2 \times \delta(\vec{p} + \vec{p}') \int d^3x e^{i\vec{p}\vec{x}} \langle \delta_{\vec{E} \cdot \vec{B}}(\tau', 0) \delta_{\vec{E} \cdot \vec{B}}(\tau'', \vec{x}) \rangle, \quad (3.28)$$

where we have used the notation $a' \equiv a(\tau')$ and $a'' \equiv a(\tau'')$.

Hence, in order to find the propagator for ϕ , we must first compute the two-point function of $\delta_{\vec{E} \cdot \vec{B}}$, find the Green function associated to the homogeneous part of equation (3.27) and solve the integral in (3.28). The details of all this calculation can be found in Appendix 1. Here we will present the final result

$$\langle \phi(\vec{p}) \phi(\vec{p}') \rangle \simeq 2 \times 10^{-6} \frac{\alpha^2 e^{4\pi\xi}}{\nu_+^2 f^2} \frac{\delta(\vec{p} + \vec{p}')}{p^3} \frac{H^4}{\xi^8} \left(\frac{2^5 \xi p}{aH} \right)^{2\nu_-}, \quad (3.29)$$

where we have defined

$$\begin{aligned} \nu_+ &\simeq \frac{\pi \alpha V'}{fH^2} \propto \frac{\alpha M_P^2}{f^2} \gg 1, \\ \nu_- &\simeq \frac{V'' f}{\pi \alpha V'} \propto \frac{1}{\alpha} \ll 1. \end{aligned} \quad (3.30)$$

Now we have all the ingredients to compute the power spectrum of the scalar perturbations \mathcal{P}_ζ . For generality, we want a result which is valid also in the case we are dealing

with a number of gauge fields $\mathcal{N} \neq 1$. In this extended scenario, the constraints we have found before remain unchanged, while the power spectrum is suppressed by a factor $1/\mathcal{N}$, since the different contributions to the two-point function of $\delta_{\vec{E}, \vec{B}}$ add incoherently. Taking the suppression into account and using also the relation $\alpha(H/\xi)^4 e^{2\pi\xi} = f|V'|/\mathcal{I}$, we get the expression

$$\mathcal{P}_\zeta \equiv \frac{p^3 H^2 \langle \phi\phi \rangle}{2\pi^2 \dot{\Phi}_0^2 \delta(\vec{p} + \vec{p}')} \simeq \frac{5 \times 10^{-2}}{\mathcal{N} \xi^2} \left(\frac{2^5 \xi p}{aH} \right)^{2\nu_-}. \quad (3.31)$$

The spectral index of the scalar perturbation is

$$n - 1 = 2\nu_- \simeq \frac{2}{\pi\alpha} \frac{f V''(\Phi_0)}{V'(\Phi_0)}. \quad (3.32)$$

Studying its behaviour with respect to V' and V'' , we notice that the sign of the former doesn't change during inflation, whereas V'' crosses zero. As a consequence, the spectrum can be either red or blue, depending on the value of Φ when the relevant scale leaved the horizon.

3.5 Scalar perturbations in natural inflation

Historically, natural inflation was the first axion model attempted, proposed as early as in 1990. In this particular setup, the potential is periodic and has the form $V(\Phi) = \Lambda^4[\cos(\Phi/f) + 1]$, which arises from nonperturbative effects and the break of the axion shift symmetry down to a subgroup $\Phi \rightarrow \Phi + (2\pi)f$. Unfortunately, the condition for inflation, i.e. the flatness requirement for the inflaton potential, is satisfied only for $f \gg M_P$, a regime which is impossible to achieve in a controlled effective field theory without having a global symmetry breaking below the Planck scale. Moreover, such large values of the axion constant seem to be not allowed in string theory.

Nevertheless, it is still possible to obtain inflation if we add precisely an interacting term to the Lagrangian like the one in (3.1). In this way, even if $f < M_P$ and the inflaton potential is steep, a part of the kinetic energy of the axion is transferred to the gauge field, effectively slowing it down to the point that the slow-roll conditions are obeyed. The transferred energy is transformed into classical fluctuations of the gauge field that, besides their dissipative effect on the inflaton, become gravitational sources and generate scalar and tensorial perturbations in the metric.

Under these assumptions, all the calculations we have done in the previous sections are still valid. In particular, we are interested in inflationary solutions where the slow-roll regime is supported by dissipation into electromagnetic modes, so ξ is governed by the transcendental equation in (3.16). Notice that, unless Φ is very close to an extremum of V (and with α not exponentially large or small), ξ grows logarithmically on $V(\Phi)$:

$$\xi \sim \frac{2}{\pi} \log \left[\frac{M_P}{\Lambda} \right], \quad (3.33)$$

and it will never be larger than $\mathcal{O}(10)$. For example, for $\Lambda \sim 10^7$ GeV, $\xi \simeq 20$.

Looking at the constraint on our solution, the condition $\alpha \gg \xi$ found previously it is mandatory in order to neglect the backreaction of the gauge field on Friedmann equation. As we mentioned before, it is violated when the inflaton approaches the minimum of the potential. In this case we enter the reheating stage, and by approximating $V(\Phi) \propto \Phi^2$ one finds that the energy density at reheating is $\sim \Lambda^4 \Phi_{RH}^2 / f^2$, so that the temperature in this phase will be of the order of $\Lambda \sqrt{\xi/\alpha}$. The expression for the reheating temperature can be used also to estimate how large ξ can be. If we want the reheating temperature to be larger than $\mathcal{O}(10^2)$ GeV in order to have enough room for baryogenesis to occur, since $\xi/\alpha \sim 10^{-2}$ there are two possible cases: a low energy scale inflation, where Λ can be as low as few TeVs, $\xi \geq 20$ and $\alpha \geq 400$, so that from the relation $\alpha \geq 2\xi N/\pi$ we see as only 30 efoldings of inflation are sufficient to solve all the Hot Big Bang theory problems; otherwise, in the opposite regime of high energy inflation, ξ can be as small as 4 with $\alpha \geq 150$ for $\Lambda \simeq 10^{16}$ GeV, in which case $N \simeq 60$ [9].

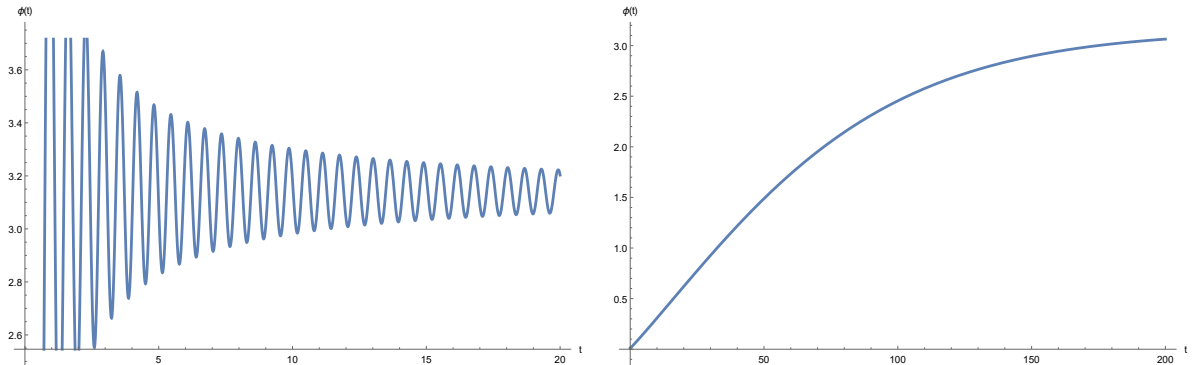


Figure 3.1: Evolution of $\phi(t)$ in natural inflation models, in the case the coupling between the inflaton and the gauge field is absent and when the backreaction is taken into account, respectively on the left and right panel. For clarity, in the left panel we consider a small temporal window.

Finally, we analyse the scalar power spectrum expression in equation (3.31). Comparing it with the COBE normalization $\mathcal{P}_\zeta = 2.5 \times 10^{-9}$, the two match only for large values of \mathcal{N} , since $\xi = \mathcal{O}(10)$. In particular, if we take $\xi \simeq 20$, then $\mathcal{N} \simeq 5 \times 10^4$ if we want perturbations with the observed amplitude. Such a large number of gauge fields might seem unattainable, but in [9] the authors claim that is possible to find tens of gauge fields in string theory, where there may be \mathcal{N} branes. Alternatively, they propose to consider a different gauge group, like $SU(\sqrt{\mathcal{N}})$, with $\sqrt{\mathcal{N}} \simeq 200$ branes. This option has the advantage that all gauge fields have automatically the same coupling constant α to the inflaton, but it requires in principle to take into account also their self-interaction, unless the gauge self-coupling is weak enough to consistently neglect this effect.

In order to visualize the effects of the coupling with the gauge field on the inflaton and support the validity of the analytical approximations we have made so far, we numerically solved both Klein-Gordon and Friedmann equations, including the backreaction only in the former. The computation was made for the choice of parameters $\alpha = 300$, $\Lambda = 10^{-3} M_P$ and $f = 0.1 M_P$. In fig. 3.1 we show the behaviour of the inflaton in the case where the coupling is absent, i.e. if we set to zero the right hand side of equation (3.15), and when the backreaction is taken into account, respectively on the left and right panel. In the free case the axion rapidly reaches an oscillatory regime, due to the periodicity of its potential, whereas the dissipative effect of the gauge field in the other case slows efficiently the inflaton, so much that the minimum of the potential is reached only after approximately 60 efoldings, as one can easily understand by inspecting the inset of figure 3.2.

The success of the inflationary process can be detected also by looking in the right

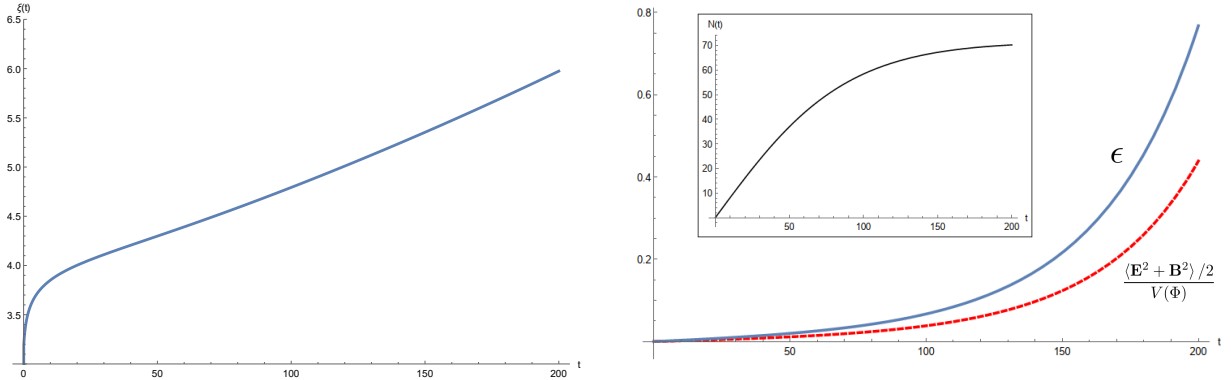


Figure 3.2: Evolution of background quantities for $\Delta = 10^{-3}M_P$, $f = 0.1M_P$, $\alpha = 300$ and $N = 10^5$, with $V(\Phi) = \Lambda^4[\cos(\Phi/f) + 1]$ and time expressed in units of M_P/Δ^2 . Left panel: evolution of $\xi(t)$. Right panel: behaviour of ϵ (in the solid blue line) and of the ratio of the energy of the gauge quanta over the energy of the inflaton (in the red, dashed curve) during inflation. The inset shows the relation between the cosmic time t and the number of efoldings N .

panel of figure 3.2, where the slow-roll parameter ϵ approaches unity only towards the end of inflation. In the same panel we depict also the ratio of the energy in gauge modes over the energy of the inflaton. As we expected, this quantity becomes significant only in the last 10 efoldings, since the production of the gauge modes grows exponentially in the axion velocity, through ξ . Hence, the backreaction of the gauge field in Friedmann equation can be safely neglected, as we have assume throughout this chapter.

Finally, in the left panel of the same figure we show the evolution of $\xi(t)$. Rather than being constant, it increases with time even if mildly, starting from $\xi \simeq 4$ and ending at $\xi \simeq 6$ after approximately 60 efoldings of inflation. This behaviour is in agreement with the logarithmic dependence in equation (3.33), which for this choice of parameters will give $\xi \simeq 4.4$.

3.6 Scalar perturbations in axion monodromy

Axion monodromy is a string-derived model based on a single axion field. The potential has the form

$$V(\Phi) = \mu^3\Phi + \Lambda^4 \cos\left[\frac{\Phi}{f}\right], \quad (3.34)$$

where the linear contribution arises from the explicit breaking of the shift symmetry when wrapping an NS5-brane on an appropriate 2-cycle, while the periodic modulation is due

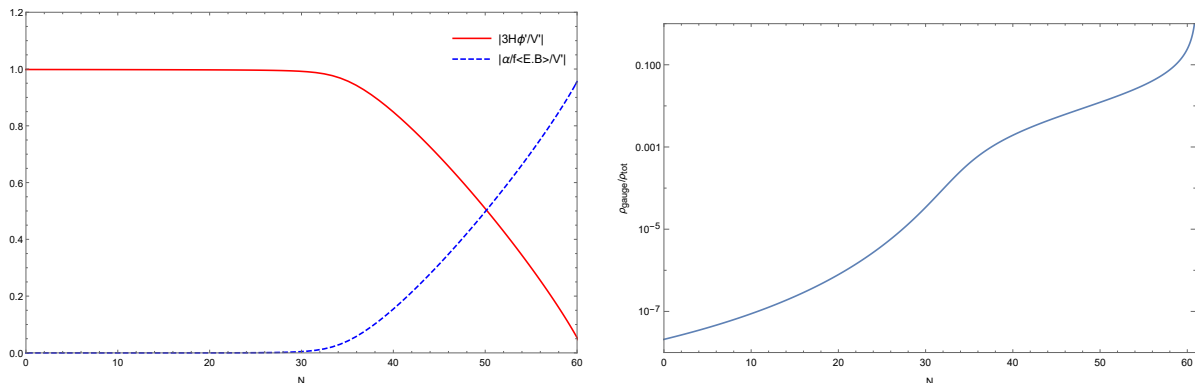


Figure 3.3: Left panel: contribution of the Hubble and gauge field friction terms to the dynamics of Φ . Right panel: relative strength of the energy density of the produced quanta; this term is neglected in the numerical evolution of Friedmann equation. Both plots were made from a linear potential.

to nonperturbative effects. The axion decay constant is bounded [12, 28] as

$$0.06\mathcal{V}^{-1/2}g_s^{1/4} < \frac{f}{M_P} < 0.9g_s, \quad (3.35)$$

where $g_s < 1$ is the string constant and $\mathcal{V} \gg 1$ is the compactification volume in string units. This bound implies then that $f \ll M_P$. The linear term in the potential dominates over the periodic modulation, so we will neglect the latter in what follows. Nevertheless, it can be shown that this correction can give rise to resonant nongaussianities which may dominate the bispectrum for $f \ll M_P$. Notice that since we now have a potential that supports inflation, we do not need to rely on dissipation to drive inflation, even though the interaction between the axion and the gauge field can enhance the production of tensor modes allowing for their detection, as we will see in the next chapter.

Considering the dynamical effects produced by the coupling between the axion and the gauge field, the main results found in the first four sections of this chapter are still valid. In particular, the backreaction of the gauge field on both Klein-Gordon and Friedmann equations becomes important only towards the end of inflation, so that at CMB/LSS scales it can be neglected. Nevertheless, an interaction of the form $\Phi F\tilde{F}$ may still have a profound impact on the cosmological fluctuations since it allows inverse decay processes $\delta A + \delta A \rightarrow \delta\Phi$ [13],[14]. This new source of inflaton fluctuations leads to a scalar power spectrum that reads, after including also the vacuum contribution,

$$\mathcal{P}_\zeta = \mathcal{P}\left(\frac{k}{k_0}\right)^{n_s-1} \left[1 + 7.5 \times 10^{-5} \mathcal{P} \frac{e^{4\pi\xi}}{\xi^6} \right], \quad (3.36)$$

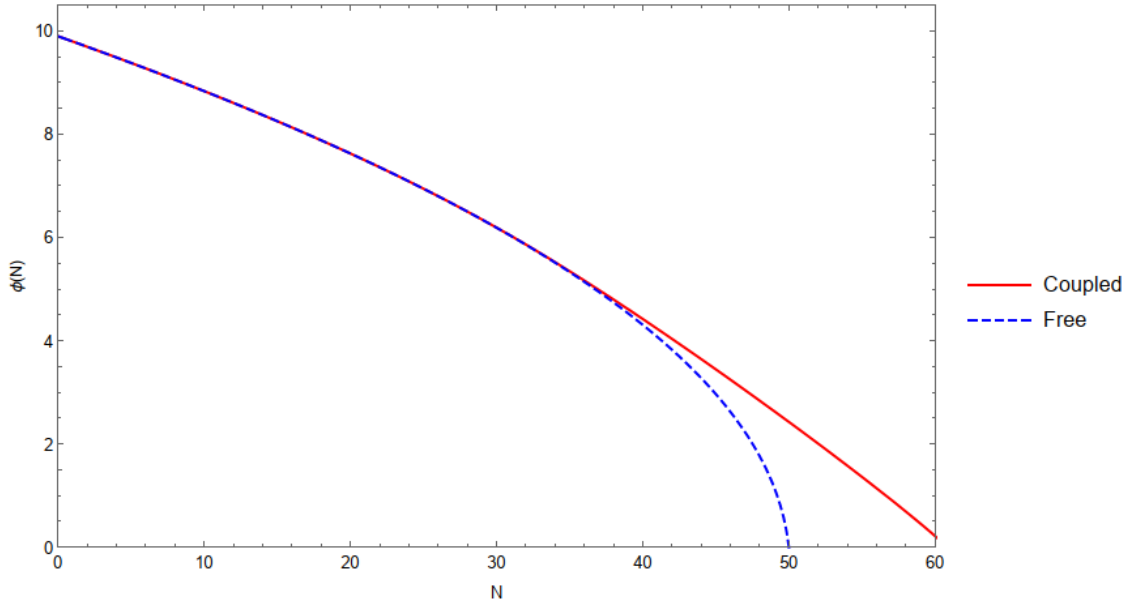


Figure 3.4: Evolution of the inflaton as a function of the number of e-foldings, starting from $|\Phi_{CMB}| = 9.9M_P$, for axion monodromy models. The red solid line ($\xi_{CMB} = 2.5$) and the green dashed line ($\xi = 0$) represents the cases with and without the coupling to gauge fields, respectively. For the first line, the value of α is chosen so to lead to observable non-Gaussianity from inverse decay. For the second line, we have shifted the number of e-foldings to make manifest that the two evolutions coincide at early times.

where $\mathcal{P}^{1/2} = H^2/(2\pi\dot{\phi})$, n_s is the spectral index and $k_0 = 0.002Mpc^{-1}$ is the pivot scale. Moreover, since as we saw ξ increases with time, the production of gauge quanta can result in an additional friction on the inflaton motion that prolongs the duration of inflation, but at the same time it may even lead to a strong backreaction regime. Therefore, we studied this possibility and checked the validity of our assumptions by means of numerical simulations.

We numerically evolve the Klein-Gordon equation and the Friedmann equation, keeping into account the backreaction term for the axion but disregarding the energy density of the gauge modes in the latter, so that we have a simple algebraic equation for H . The right panel of figure 3.3 allows to check that this last assumption is valid. Indeed, the ratio between the energy density of the gauge quanta and the total energy of the system becomes dangerously close to unity only at the very end of inflation. The parameters are chosen so that the results for the power spectrum found previously apply also in this case. In particular, starting from the slow-roll form of the Klein-Gordon and

Freidmann equations in (2.10) and (2.11), we can derive a relation between the initial values of ξ and Φ at the CMB scale and the ratio α/f :

$$\xi|_{\Phi_{CMB}} = 2.5 \rightarrow \frac{\alpha}{f} = 5 \frac{|\Phi_{CMB}|}{M_P^2}. \quad (3.37)$$

The mass scale μ was instead derived requiring COBE normalization for the scalar power spectrum $\mathcal{P}_\zeta^{1/2} = H^2/(2\pi\dot{\phi}) \simeq 5 \cdot 10^{-5}$.

In figure 3.4 we show the evolution of the inflaton as a function of the number of efoldings for two different values: $\xi_{CMB} = 2.5$ and $\xi = 0$, i.e. the free case with no coupling between the axion and the gauge field. Given the same initial value of the field at the CMB scale, the backreaction of the gauge modes on the background evolution becomes noticeable only in the last ~ 25 efoldings of inflation, while it is completely negligible at earlier times. In particular, the two trajectories reaches the minimum of the potential with a difference of ~ 10 efoldings, showing that the backreaction has successfully increased the duration of inflation.

The effect of the gauge quanta on the dynamics of the inflaton during the last ~ 25 efoldings is visible also in the left panel of figure 3.3, where we plot the evolution of the two friction terms in the axion equation as a function of N . The standard Hubble friction controls the early stages of inflation, but the backreaction of the produced gauge quanta gradually increases its contribution until it completely dominates the evolution of the system. Namely, in the last ~ 10 efoldings the system approaches the strong backreaction regime, where a more sophisticated numerical method is required, see [16].

Chapter 4

Tensor perturbations and Power Spectrum

Until now we have seen how the coupling between the axion-like inflaton and the gauge field allows the former to slow down when rolling down its potential, while providing enough energy to the latter to produce classical fluctuations. These particles are then sources for the gravitational field, leading to scalar and tensor perturbations. The scalar power spectrum was computed in the last chapter; here we will focus in the production of tensor modes and in their power spectrum. Again, we will first present the subject in full generality before specializing our results for particular models.

4.1 Generation of tensor modes

Let us start from the form of the tensorial part of the perturbed metric as a function of conformal time τ

$$ds^2 = a^2(\tau)[-d\tau^2 + (\delta_{ij} + h_{ij})dx^i dx^j], \quad (4.1)$$

where the tensor modes h_{ij} are traceless and transverse, i.e. $h_i{}^i = h_{ij,j} = 0$. Introducing the transverse traceless projector

$$\Pi_{ij}{}^{lm} = \Pi_i{}^l \Pi_j{}^m - \frac{1}{2} \Pi_{ij} \Pi^{lm}, \quad (4.2)$$

with $\Pi_{ij} = \delta_{ij} - \partial_i \partial_j / (\partial_i \partial^i) = \delta_{ij} - \partial_i \partial_j / \Delta$, and the spatial part of the energy-momentum tensor for the gauge field

$$T_{ij}^{\text{EM}} = -a^2(E_i E_j + B_i B_j) + \frac{a^2}{2}(E^2 + B^2)\delta_{ij}, \quad (4.3)$$

the equation of motion for the gravitational waves h_{ij} reads

$$h_{ij}'' + 2\frac{a'}{a}h_{ij}' - \Delta h_{ij} = \frac{2}{M_P^2} \Pi_{ij}{}^{lm} T_{lm}^{\text{EM}}. \quad (4.4)$$

From now on, we will ignore the second term proportional to the delta function in the definition of the energy-momentum tensor, since we are interested only on its traceless and transverse part.

Moving to momentum space, it is customary to project h_{ij} into positive and negative helicity modes

$$h^{ij}(\vec{k}) = \sqrt{2} \sum_{\lambda=\pm} \epsilon_{\lambda}^i(\vec{k}) \epsilon_{\lambda}^j(\vec{k}) h_{\lambda}(\tau, \vec{k}), \quad (4.5)$$

where the amplitude $h_{\lambda}(\vec{k})$ can be found by using the polarization tensors $\Pi_{\pm}^{ij}(\vec{k}) = \epsilon_{\mp}^i(\vec{k}) \epsilon_{\mp}^j(\vec{k}) / \sqrt{2}$, so that $h_{\pm}(\vec{k}) = \Pi_{\pm}^{ij}(\vec{k}) h_{ij}(\vec{k})$. Here the helicity vectors ϵ_{\pm}^i are defined such that $k_i \epsilon_{\pm}^i = 0$, $\varepsilon_{abc} k^b \epsilon_{\pm}^c = \mp i k \epsilon_{\pm}^a$, $\epsilon_{\pm}^i \epsilon_{\mp}^i = 1$ and $\epsilon_{\pm}^i \epsilon_{\pm}^i = 0$. Now we promote the functions h_{\pm} to operators. Neglecting for the moment the homogeneous part of the equation of motion for h_{ij} in (4.4), we first introduce the Green function for the operator $d^2/d\tau^2 - (2/\tau)d/d\tau + k^2$,

$$G_k(\tau, \tau') = \frac{1}{k^3 \tau'^2} [(1 + k^2 \tau \tau') \sin[k(\tau - \tau')] + k(\tau' - \tau) \cos[k(\tau - \tau')]] \quad (4.6)$$

for $\tau > \tau'$, while $G_k(\tau < \tau') = 0$. Then, using the property $\Pi_{\pm}^{ij} \Pi_{ij}^{lm} = \Pi_{\pm}^{lm}$, the expression for h_{\pm} is

$$\hat{h}_{\pm}(\vec{k}) = -\frac{2H^2}{M_P^2} \int d\tau' G_k(\tau, \tau') \tau'^2 \int \frac{d^3 q}{(2\pi)^{3/2}} \Pi_{\pm}^{lm}(\vec{k}) \times \quad (4.7)$$

$$\times \left[\hat{A}'_l(\vec{q}, \tau') \hat{A}'_m(k \vec{-} q, \tau') - \varepsilon_{lab} q_a \hat{A}'_b(\vec{q}, \tau') \varepsilon_{mcd} (k_c - q_c) \hat{A}'_m(k \vec{-} q, \tau') \right], \quad (4.8)$$

where we have substituted in the definition of T_{ij}^{EM} the expressions of \vec{E} and \vec{B} in terms of the four-potential $A(\vec{k}, \tau)$.

As we discussed in the previous chapter, only the A_+ mode is amplified by the rolling inflaton while A_- can be set to zero. Moreover, since the production of tensor modes is efficient only when $(8\xi)^{-1} \ll |k\tau| \ll 2\xi$, we can use the approximated form in equation (3.11) for the positive-helicity gauge mode. By applying Wick's theorem, one can find the two-point function for the helicity- λ graviton (see Appendix B for more details in the calculation):

$$\begin{aligned} \langle h_{\lambda}(\vec{k}) h_{\lambda}(\vec{k}') \rangle &= \frac{H^4 \xi}{4\pi^3 M_P^4} e^{4\pi\xi} \delta(\vec{k} + \vec{k}') \int d\tau' d\tau'' |\tau'|^{3/2} |\tau''|^{3/2} G_k(\tau, \tau') G_k(\tau, \tau'') \times \quad (4.9) \\ &\times \int d^3 \vec{q} |\epsilon_{-\lambda}^i(\vec{k}) \epsilon_{+}^i(\vec{q})|^2 |\epsilon_{-\lambda}^j(\vec{k}) \epsilon_{+}^j(k \vec{-} q)|^2 \sqrt{|k \vec{-} q|} \sqrt{q} e^{-2\sqrt{2}\xi(\sqrt{|\tau'|} + \sqrt{|\tau''|})(\sqrt{q} + \sqrt{|k \vec{-} q|})}. \end{aligned} \quad (4.10)$$

Notice that the result depends on both the propagators, through the Green functions, and on the amplitude of the gauge field and on the helicity of the graviton. In the large

scale limit $-k\tau \rightarrow 0$, the integral above can be computed numerically, but here we prefer to use a semi-analytical approximation valid for $\xi \gtrsim 3$:

$$\langle h_+(\vec{k})h_+(\vec{k}') \rangle \simeq 8.6 * 10^{-7} \frac{H^4}{M_P^4} \frac{e^{4\pi\xi}}{\xi^6} \frac{\delta(\vec{k} + \vec{k}')}{k^3}, \quad (4.11)$$

$$\langle h_-(\vec{k})h_-(\vec{k}') \rangle \simeq 1.8 * 10^{-9} \frac{H^4}{M_P^4} \frac{e^{4\pi\xi}}{\xi^6} \frac{\delta(\vec{k} + \vec{k}')}{k^3}. \quad (4.12)$$

As we can see, both the left- and right-handed tensor modes spectra are scale invariant, but thanks to the parity-violating nature of the system, they differ by a factor $\sim 10^3$. The discrepancy comes from the term $|\epsilon_{-\lambda}^i(\vec{k})\epsilon_+^i(\vec{q})|^2|\epsilon_{-\lambda}^j(\vec{k})\epsilon_+^j(\vec{k}-\vec{q})|^2$. In particular, using the properties of the helicity vectors, when $|\vec{q}| \ll |\vec{k}|$ the correlator vanishes for $\lambda = -$ but remains finite for $\lambda = +$, a result which can be easily explained from a physical point of view by noticing that for small transverse momentum, conservation of angular momentum does not allow two positive-helicity photons to generate a negative-helicity graviton.

As we did for the scalar perturbations, our final goal is to have the tensor mode power spectrum, which can be then easily compared with experimental results. Its definition is analogous to the one we provided in the curvature perturbations:

$$\mathcal{P}^{t,\pm} = \frac{k^3}{2\pi^2} |h_{\pm}(\vec{k})|^2. \quad (4.13)$$

In addition to our results in equations (4.11) and (4.12), we must also take into account the parity-symmetric contribution to gravitons coming from the homogeneous part of the equation of motion (4.4), i.e. the gravitational waves generated by the standard amplification of vacuum fluctuations in a de Sitter spacetime. Therefore, the final result reads

$$\mathcal{P}^{t,+} = \frac{H^2}{\pi^2 M_P^2} \left(1 + 8.6 \times 10^{-7} \frac{H^2}{M_P^2} \frac{e^{4\pi\xi}}{\xi^6} \right), \quad (4.14)$$

$$\mathcal{P}^{t,-} = \frac{H^2}{\pi^2 M_P^2} \left(1 + 1.8 \times 10^{-9} \frac{H^2}{M_P^2} \frac{e^{4\pi\xi}}{\xi^6} \right). \quad (4.15)$$

In order to compare our results with the sensitivity of interferometers, it is convenient to introduce the fractional energy density per logarithmic wavenumber interval, in units of the critical density ρ_{crit} ,

$$\Omega_{\text{GW},0} = \frac{1}{\rho_{\text{crit},0}} \frac{\partial \rho_{\text{GW},0}}{\partial \ln k} = \frac{8\pi G}{3H_0^2} \frac{\partial \rho_{\text{GW},0}}{\partial \ln k}, \quad (4.16)$$

where the label 0 refers to quantities evaluated today, while no label means the end of inflation. Using the fact that both radiation and GW energy densities scales like a^{-4} , we

can back evolve the density parameter to the end of inflation, when our results for both the two-point function and the tensor power spectrum are still valid. Indeed, one can write

$$\Omega_{\text{GW},0} = \frac{1}{\rho_{\text{crit},0}} \frac{\partial \rho_{\text{GW},0}}{\partial \ln k} = \frac{1}{\rho_{\text{crit},0}} \frac{a^4}{a_0^4} \frac{\partial \rho_{\text{GW}}}{\partial \ln k} = \frac{1}{\rho_{\text{crit},0}} \frac{\rho_{\gamma,0}}{\rho_{\gamma}} \frac{\rho_{\text{GW}}}{\partial \ln k} = \quad (4.17)$$

$$= \Omega_{\gamma,0} \frac{1}{\rho_{\gamma}} \frac{\partial \rho_{\text{GW}}}{\partial \ln k} = \Omega_{\gamma,0} \frac{1}{\rho_{\text{crit}}} \frac{\partial \rho_{\text{GW}}}{\partial \ln k}, \quad (4.18)$$

where in the last step we have used $\rho_{\gamma} = \rho_{\text{crit}}$ at the end of inflation, i.e. at the beginning of RD era. The vacuum expectation value of the gravitational wave energy density is given by

$$\langle 0 | \rho_{\text{GW}} | 0 \rangle = \langle 0 | \frac{1}{64\pi G} \frac{(h'_{ij})^2 + (\vec{\nabla} h_{ij})^2}{a^2} | 0 \rangle = \frac{1}{64\pi G} \int_0^{\text{inf}} \frac{k^3}{2\pi^2} \frac{|h_{\pm}(\vec{k})'|^2 + k^2 |h_{\pm}(\vec{k})|^2}{a^2} \frac{dk}{k}. \quad (4.19)$$

Inserting this expression in equation (4.18) and using the property $|h_{\pm}(\vec{k})'|^2 = k^2 |h_{\pm}(\vec{k})|^2$, valid for modes which have re-entered the horizon after inflation, the final result for the density parameter is

$$\Omega_{\text{GW},0} = \Omega_{\gamma,0} \frac{8\pi G}{3H^2} \frac{2k^2}{64\pi G} \frac{k^3}{2\pi^2} (|h_+|^2 + |h_-|^2) = \frac{\Omega_{\gamma,0}}{12} \frac{k^2}{a^2 H^2} (\mathcal{P}^{t,+} + \mathcal{P}^{t,-}), \quad (4.20)$$

where today density parameter for radiation has value $\Omega_{\gamma,0} = \rho_{\gamma,0}/3H_0^2 M_P^2 \simeq 8.6 \cdot 10^{-5}$ and the fraction $k^2/(aH)^2$ can be set equal to 1 at horizon crossing. It is useful to plot $\Omega_{\text{GW},0}$ as a function of frequency $f = k/2\pi$, which can on the other hand be related to the number of e-foldings via the relation

$$N - N_{\text{CMB}} = \ln a - \ln a_{\text{CMB}} = \ln \frac{a}{a_{\text{CMB}}} = \ln \frac{k_{\text{CMB}}}{k} = \ln \frac{k_{\text{CMB}}}{0.002 \text{Mpc}^{-1}} - \ln \frac{k}{0.002 \text{Mpc}^{-1}} = \quad (4.21)$$

$$= \ln \frac{k_{\text{CMB}}}{0.002 \text{Mpc}^{-1}} - \ln \frac{2\pi f}{0.002 \text{Mpc}^{-1}} = \ln \frac{k_{\text{CMB}}}{0.002 \text{Mpc}^{-1}} - 44.9 - \ln \frac{f}{10^2 H_z}. \quad (4.22)$$

Although the results that we have obtained are independent from the actual form of the inflaton potential, some constraints need to be applied to the model. First of all, we have to impose COBE normalization for the scalar perturbations power spectrum, which we rewrite for convenience as

$$\mathcal{P}_{\zeta} = \frac{H^2}{8\pi^2 \epsilon M_P^2} \left[1 + 9.5 \times 10^{-7} \frac{H^2}{\epsilon M_P^2} \frac{e^{4\pi\xi}}{\xi^6} \right]; \quad (4.23)$$

such condition then reads $\mathcal{P}_\zeta = \mathcal{P}_\zeta^{\text{obs}} = 2.5 \times 10^{-9}$. In addition to this, the strongest constraint comes from the requirement that nongaussianities are within the limits set by observations. The parameter which encodes departure from gaussianity is the three-point correlation function, and it can be shown via similar calculations to the ones we already performed that in our setup it has maximal amplitude for equilateral configurations, where

$$f_{\text{NL}}^{\text{equil}} \simeq 8.9 \times 10^4 \frac{H^6}{\epsilon^3 M_P^6} \frac{e^{6\pi\xi}}{\xi^9}. \quad (4.24)$$

Using the expression for the curvature perturbations power spectrum in (4.23) in the equation above, from the current Planck 2018 limit [25] $f_{\text{NL}}^{\text{equil}} = -26 \pm 47$ at 68% CL we derive the upper bound $\xi < 2.527$.

4.2 Tensor perturbations in natural inflation models

In a natural inflation scenario, for such small values of ξ and for $H \lesssim 10^{-4} M_P$ parity violation in the CMB is undetectable while respecting the constraints from nongaussianities, as one can see by considering the net handedness of the tensor modes through the parameter

$$\Delta\chi \equiv \frac{\mathcal{P}^{t,+} - \mathcal{P}^{t,-}}{\mathcal{P}^{t,+} + \mathcal{P}^{t,-}} = \frac{4.3 \times 10^{-7} \frac{e^{4\pi\xi}}{\xi^6} \frac{H^2}{M_P^2}}{1 + 4.3 \times 10^{-7} \frac{e^{4\pi\xi}}{\xi^6} \frac{H^2}{M_P^2}}. \quad (4.25)$$

Indeed, a simple calculation made with $\xi_{\text{CMB}} = 2.527$ and $H = 10^{-4} M_P$ leads to a chirality parameter $\Delta\chi = 0.00095$ at the CMB scales, which is too small to be verified by any current and future experiments. Therefore, the model needs to be modified for parity violation to be detected while complying with the other observations. In [10], two possible ways are proposed.

The first possibility is to consider a second scalar field, a curvaton, that accounts for the majority of the density perturbations and has a gaussian statistics. Denoting by $\delta < 1$ the fraction of contribution from equation (4.23) to the observed $\mathcal{P}_\zeta^{\text{obs}}$, so that $\mathcal{P}_\zeta^\phi = 2.5\delta \times 10^{-9}$, it is easy to see that if $f_{\text{NL}}^{\text{equil}} \simeq 8400\delta^{3/2}$ the $\delta \simeq 0.01$ is sufficient to make f_{NL} compatible with observations for all values of ξ . In the limit $\xi \gg 1$, the tensor modes are fully chiral ($\Delta\chi \simeq 1$), and the tensor-to-scalar ratio $r = (\mathcal{P}^{t,+} + \mathcal{P}^{t,-})/\mathcal{P}_\zeta^{\text{obs}}$ can be written as $r \simeq 7.2 \times \delta \times \epsilon^2$. Detectable parity violation in the spectrum of gravitational waves can be reached for r as small as ~ 0.009 , which corresponds to $\epsilon \gtrsim 1/3$. Though this large value of the slow-roll parameter is unusual in standard models of inflation, in curvaton models the only requirement is that $\epsilon \lesssim 1$ for inflation to occur.

Another possibility is to consider a system with several gauge fields, all with the same coupling to the inflaton, as we did in the case of the scalar power spectrum. In this way, equations (4.14),(4.15),(4.23) and (4.25) are modified by multiplying by \mathcal{N} their ξ -dependent parts, as well as the expression for f_{NL} in which a factor of \mathcal{N} is added. In

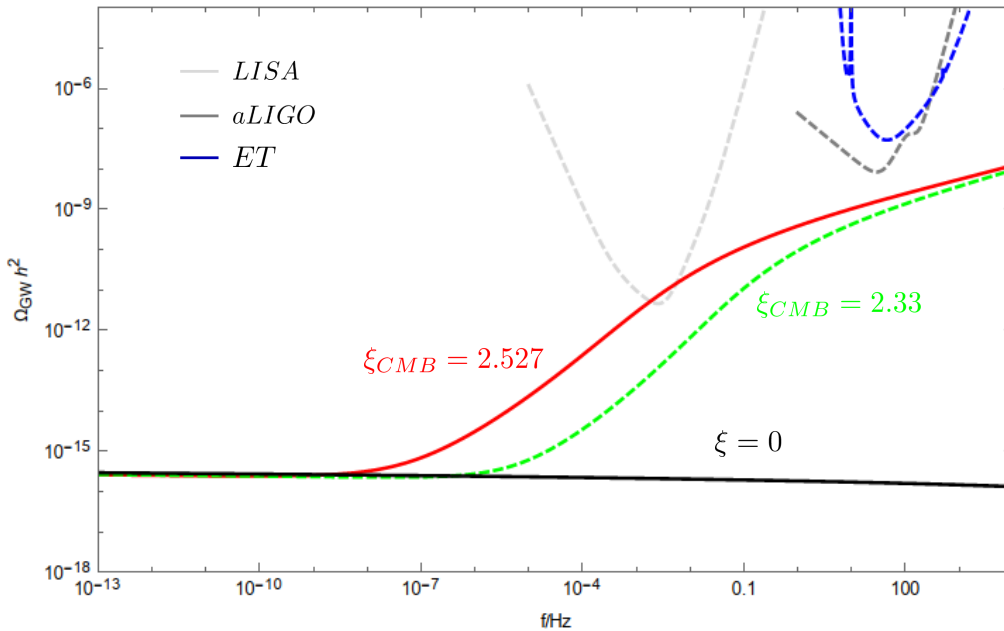


Figure 4.1: $\Omega_{\text{GW}} h^2$ as function of the frequency f in the case of a linear potential for $\xi_{\text{CMB}} = 0; 2.33; 2.527$. We have required $N = 60$ e-foldings of observable inflation. For reference we also show the sensitivity curves of LISA, Advanced LIGO/VIRGO and Einstein Telescope.

the regime of large ξ , once we impose COBE normalization the three point function scales as $1/\sqrt{\mathcal{N}}$. As a consequence, by setting $\mathcal{N} \simeq 10^5$ the constraint from nongaussianities is satisfied for all values of ξ . As stated in the previous chapter, such a large number of gauge field can arise in string theory, where string compactifications with thousands of degrees of freedom is common, according to [9].

4.3 Gravitational waves from axion monodromy inflation

Instead of introducing modified natural inflation models to have parity-violating gravitational waves which can be detected by interferometers, axion monodromy may constitute a better solution.

As we saw, since the gauge modes get amplified at late times, the tensor power spectrum grows exponentially only towards the end of inflation, specifically in the last ~ 10 efoldings. Hence, gravitational waves detectable by interferometers arise only

on small scales when the backreaction of the gauge quanta becomes important. The dissipation effect of the gauge modes acts directly on the scalar cosmological fluctuations, leading to a scalar power spectrum of the form

$$\mathcal{P}_\zeta \simeq \mathcal{O}(10^{-2}) \frac{1}{\xi^2}, \quad (4.26)$$

as we derived in section 4 of the previous chapter. Although curvature fluctuations on small scales are much larger than on CMB scales, a perturbative analysis of gravitational waves, as we did before, is still justified for small values of ξ .

The numerical result for the density parameter of gravitational waves as a function of their frequency is plotted in figure 4.1 for 3 different values of ξ at the CMB scale: $\xi|_{CMB} = 2.527$, the maximum values allowed by nongaussianities, $\xi|_{CMB} = 2.33$ and $\xi|_{CMB} = 0$, corresponding to the free case. The computation was done similarly to what was done in the previous chapter, taking into account the backreaction on the inflaton field but not on H and defining the ratio α/f and μ as in (3.37) and below. Moreover, we assumed $N_{CMB} = 60$ for fluctuations at the CMB scales.

Notice that, for a fixed $\xi|_{CMB} \neq 0$ there are three different phases in the gravitational signal. For small frequencies, only the vacuum fluctuations are present in the spectrum; as the frequency increases, there is first a fast growth due to the inverse decay contribution and then a phase with a reduced increase rate related to the strong backreaction at late times. In addition to this, a second effect which is clearly visible in figure 4.1 is that for larger $\xi|_{CMB}$ the whole signal is shifted towards lower frequencies, since there are more gauge quanta that contribute to the backreaction, effectively increasing the number of efoldings at the end of inflation. The two effects act in opposite directions, but the latter dominates over the former, so that the net result is an increase in the signal thanks to the strong backreaction.

Despite the enhancement in the parity violating gravitational waves signal due to the backreaction of the gauge modes on the scalar field at late times, figure 4.1 shows that this effect is not sufficient for detection with interferometers. The maximum value of $\xi|_{CMB}$ allowed by nongaussianities is barely sufficient to marginally superimpose the gravitational waves signal and LISA sensitivity curve, whereas the signal is totally absent for advanced LIGO and Einstein Telescope.

4.4 Chiral gravitational waves for a step-like potential

Axion monodromy fails in producing detectable chiral gravitational waves at interferometers scales, at least in its simplest version, because the tensor perturbations are efficiently produced only in the last ~ 10 efoldings and therefore the frequency of their signal is too high for current interferometers. One possible solution is to slightly change the linear potential we considered before by adding a step via an hyperbolic tangent. The generation of gravitational waves increases exponentially in ξ , which in turn is directly related to the axion's velocity. In correspondence of the step, the inflaton velocity first increases and then drops thanks to a positive and negative acceleration, respectively. Gauge modes production can therefore be localized only within the time period in which the axion is rolling down the step.

Indeed, if we take a potential of the form

$$V(\phi) = \mu^3 \times \left(|\phi| - \delta \tanh \left[\frac{\phi - \phi_0}{\Delta} \right] + \delta \right) \quad (4.27)$$

then by suitably choosing the parameters δ , Δ and ϕ_0 we can force the production of gauge quanta and tensor perturbations at earlier times and at the same time have enough inflation later to decrease the frequency of the gravitational waves. Here, ϕ_0 sets the position of the step, Δ its width and δ how steep it is, and they are all expressed in units of M_P .

In order to explore this model, we numerically solved Klein-Gordon equation for the inflaton, where we took into account the backreaction term from the gauge modes, together with the backreaction-free Friedmann equation. The system is governed by 7 parameters, namely f , α , μ , ϕ_{CMB} , ϕ_0 , δ and Δ , but not all of them are independent. Indeed, the ratio α/f is related to the value of ξ at the CMB scale through the relation

$$\xi_{CMB} = -\frac{\alpha}{2f} \frac{V'}{V} = -\frac{\alpha}{2f} \times \frac{\frac{|\phi_{CMB}|}{\phi_{CMB}} - \frac{\delta}{\Delta} \cosh \left[\frac{\phi_{CMB} - \phi_0}{\Delta} \right]^{-2}}{|\phi_{CMB}| - \delta \tanh \left[\frac{\phi_{CMB} - \phi_0}{\Delta} \right] + \delta}, \quad (4.28)$$

while the mass scale μ is determined once again by requiring COBE normalization for the scalar power spectrum:

$$\mathcal{P}_\zeta^{\text{obs}} = \frac{V^3}{12\pi^2 V'^2} = \frac{\left(\mu^3 \times \left(|\phi_{CMB}| - \delta \tanh \left[\frac{\phi_{CMB} - \phi_0}{\Delta} \right] + \delta \right) \right)^3}{12\pi^2 \left(\mu^3 \times \left(\frac{|\phi_{CMB}|}{\phi_{CMB}} - \frac{\delta}{\Delta} \cosh \left[\frac{\phi_{CMB} - \phi_0}{\Delta} \right]^{-2} \right) \right)^2}. \quad (4.29)$$

Moreover, the values of f and ξ_{CMB} can be fixed before the simulation; by requiring to have $N_{CMB} = 60$ it is also possible to determine ϕ_{CMB} via an iterative process. The choice

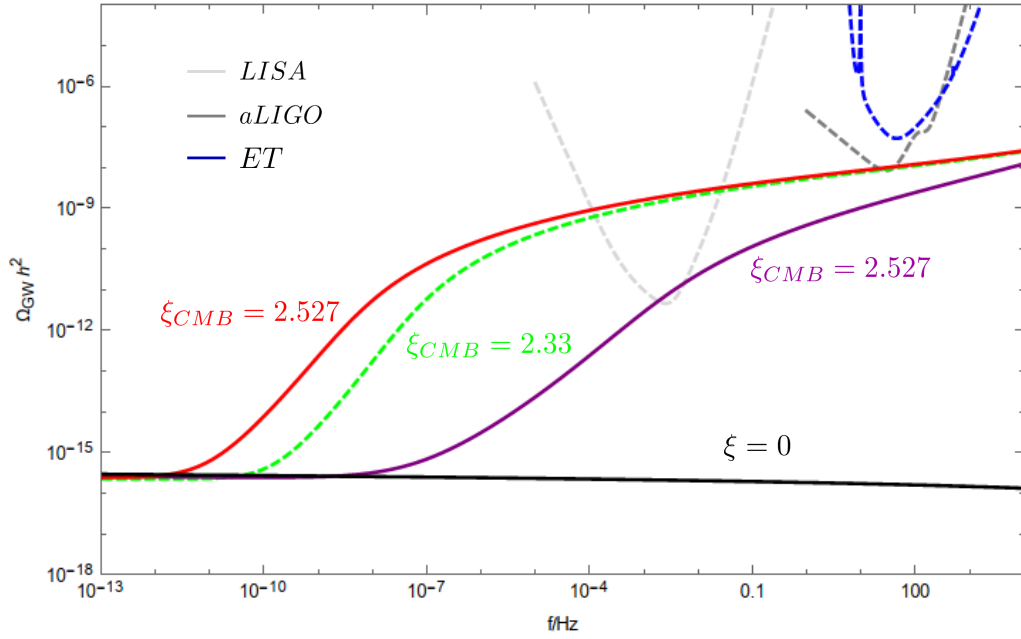


Figure 4.2: $\Omega_{\text{GW}} h^2$ as a function of the frequency f in the case of a linear potential with a step modulation given by an hyperbolic tangent, for $\xi_{\text{CMB}} = 0; 2.33; 2.527$, $\delta = 3.5$ and $\Delta = 3$. We have required $N = 60$ e-foldings of observable inflation. For reference we also show the sensitivity curves of LISA, Advanced LIGO/VIRGO and Einstein Telescope. As a reference, in purple we show the gravitational signal for $\xi_{\text{CMB}} = 2.527$ for plain axion monodromy.

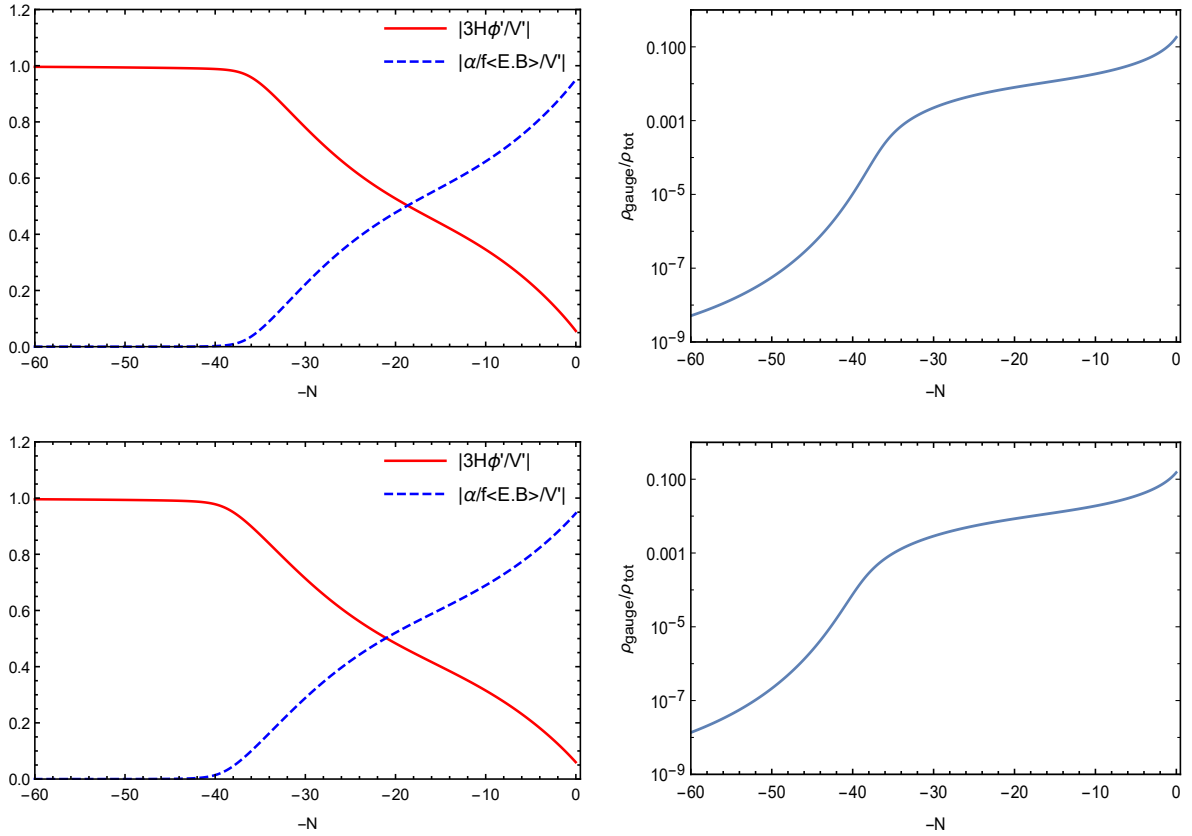


Figure 4.3: Friction terms in Klein-Gordon equation for ϕ (on the left panel) and relative strength of the energy density of the produced quanta (on the right panel) for $\xi_{CMB} = 2.33$ and $\xi_{CMB} = 2.527$, respectively on the top and on the bottom, for a potential of the form (4.27). For both values of ξ_{CMB} the contribution from the backreaction to Friedmann equation was neglected and the parameters have values $\Delta = 3$ and $\delta = 3.5$.

for ϕ_0 can be made according to when during inflation we need to enhance the production of gravitational waves, as we will discuss in the following. In the end, the values for α and μ can be numerically obtained by equations (4.28) and (4.29), respectively, and depends only on the choice for δ and Δ .

There are two possible regimes, according to the order of magnitude of Δ . In the case the step given by the hyperbolic tangent is mild, i.e. for super-Planckian values of $\Delta \gtrsim 2$, the model we designed gives a promising result for $\xi_{CMB} = 2.527$ and $\xi_{CMB} = 2.33$, as can be seen in figure 4.2. The characteristic growth of the density parameter is still present, but the whole spectrum is successfully shifted towards lower frequencies, so that LISA may be able in future to detect strong signals of chiral gravitational waves. On the other hand, advanced LIGO and Einstein Telescope are still blind since for the greater frequencies in which they operates the signal is still too low. In figure 4.3 we control the contributions from the two possible backreactions, for both values of ξ_{CMB} . In the left panel we plot the two friction terms in the Klein-Gordon equation. Having set ϕ_0 at 25 efoldings before the end of inflation, we see as the gauge quanta start dissipating the inflaton energy about 10 efoldings earlier with respect to what was found for plain axion monodromy. As we expected, the strong backreaction regime already dominates over the standard Hubble friction term at ~ 20 efoldings before the end of inflation, doing the trick to increase at earlier times the tensor power spectrum. In the right panel of figure 4.3, instead, we show the relative energy contained in the gauge quanta. Although it reaches order of unity only at the very end of inflation, the large plateau between ~ 30 and ~ 10 efoldings before inflation ends, where $\rho_{\text{gauge}}/\rho_{\text{tot}} \sim 0.01$, might give rise to a cumulative effect that would jeopardise our assumption of no backreaction in Friedmann equation.

For sub-Planckian values of Δ , i.e. $\Delta \lesssim 0.8$, the step becomes very steep and the shape of the density parameter as a function of the frequency changes drastically. Instead of the two-slope increase, as Δ gets smaller and smaller a peak emerges from the vacuum signal and gets progressively enhanced. After this hill, the signal doesn't come back to the original value, but after a drop which depends on the steepness of the modulation in the potential, it continues to grow with the same behaviour we saw in the case Δ is super-Planckian and in the axion monodromy model, due to the backreaction effect of the gauge field. This particular behaviour can be physically explained by taking into account the form of the potential. Indeed, when the inflaton reaches the step it experiences a sudden, strong acceleration; its velocity increases dramatically in a small period of time, leading to an overproduction of gauge modes, hence of chiral gravitational waves. Once the scalar field reaches the end of the step, the negative acceleration slows it down and the signal gets damped, but not completely.

A visual representation of the dependence of both the maximum value of Ω_{GW} at the peak and the corresponding frequency f as a function of δ and Δ are depicted in figure 4.4 and 4.5, respectively. The same values are also reported in table 4.1, for clarity. As a function of Δ , the peak of the hill grows as Δ gets smaller, as one expect since the inflaton

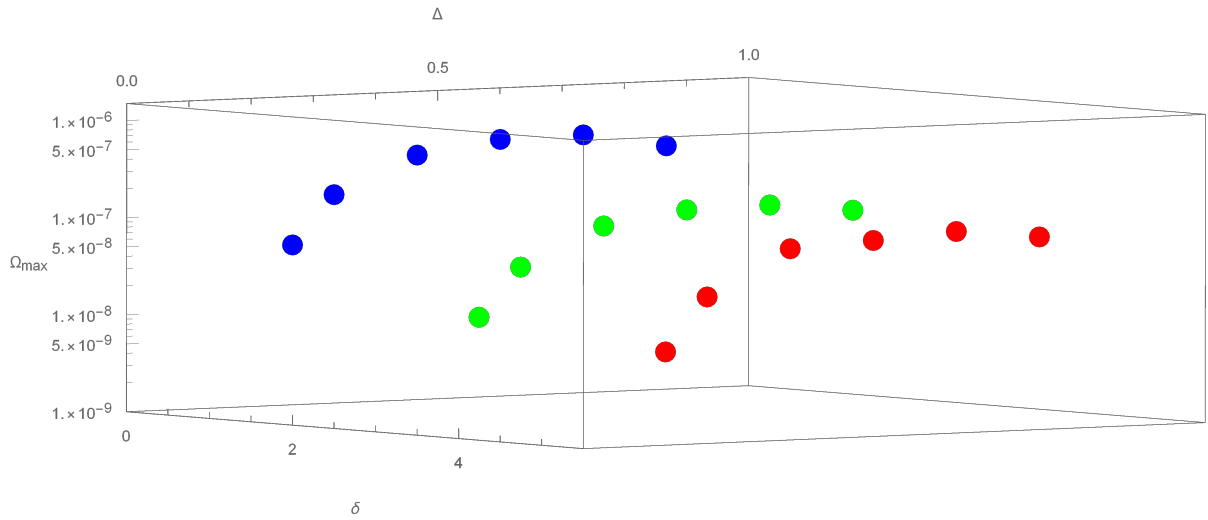


Figure 4.4: Value of $\Omega_{\text{GW}}h^2$ at the peak of the hill region for different choices of the parameters δ and Δ . To each colour corresponds a fixed value of Δ , namely blue, green and red for $\Delta = 0.2; 0.5; 0.8$, respectively.

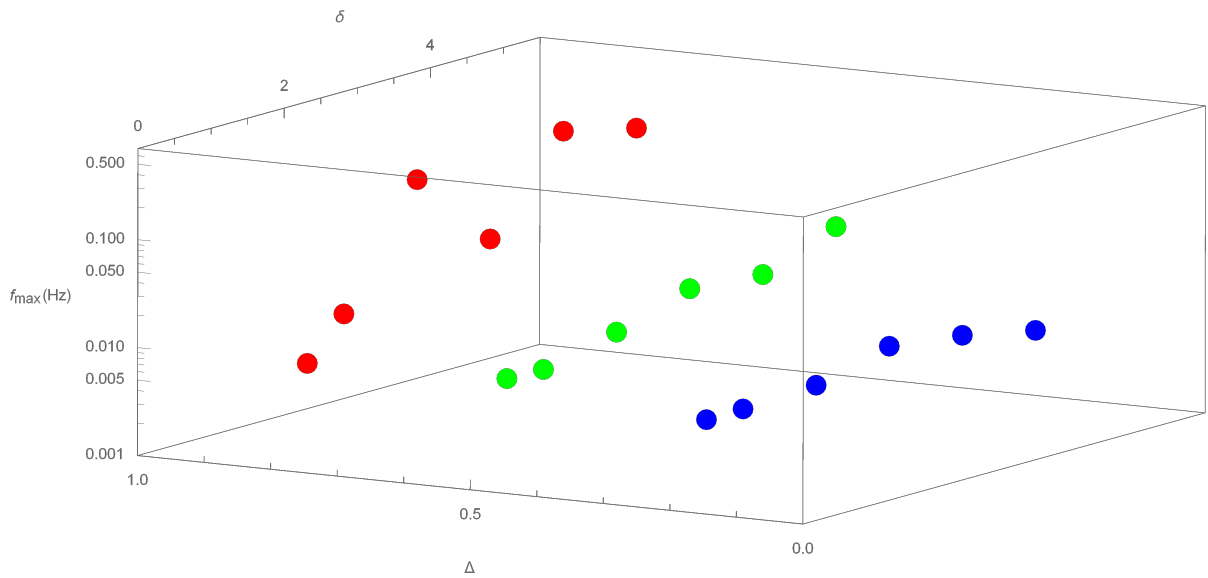


Figure 4.5: Frequency of the maximum of the hill region for different choices of the parameters δ and Δ . To each colour corresponds a fixed value of Δ , namely blue, green and red for $\Delta = 0.2; 0.5; 0.8$, respectively.

δ	Δ	Ω_{\max}	f_{\max}
5	0.8	$8.53816 \cdot 10^{-8}$	0.167557
5	0.5	$1.935352 \cdot 10^{-7}$	0.0317491
5	0.2	$1.074333 \cdot 10^{-6}$	0.00538124
4	0.8	$8.28382 \cdot 10^{-8}$	0.241711
4	0.5	$1.87047 \cdot 10^{-7}$	0.0175859
4	0.2	$1.188560 \cdot 10^{-6}$	0.00745644
3	0.8	$5.70893 \cdot 10^{-8}$	0.0372875
3	0.5	$1.42030 \cdot 10^{-7}$	0.0200096
3	0.2	$9.100469 \cdot 10^{-7}$	0.00909497
2	0.8	$3.999176 \cdot 10^{-8}$	0.203672
2	0.5	$8.264101 \cdot 10^{-8}$	0.0121956
2	0.2	$5.352503 \cdot 10^{-7}$	0.00609385
1	0.8	$1.086502 \cdot 10^{-8}$	0.0178734
1	0.5	$2.655666 \cdot 10^{-8}$	0.00846694
1	0.2	$1.784154 \cdot 10^{-7}$	0.0056523
0.5	0.8	$2.721432 \cdot 10^{-9}$	0.00771076
0.5	0.5	$7.460002 \cdot 10^{-9}$	0.00865278
0.5	0.2	$4.995847 \cdot 10^{-8}$	0.00558216

Table 4.1: Value of $\Omega_{\text{GW}}h^2$ at the peak of the hill region and corresponding frequency for different choices of the parameters δ and Δ .

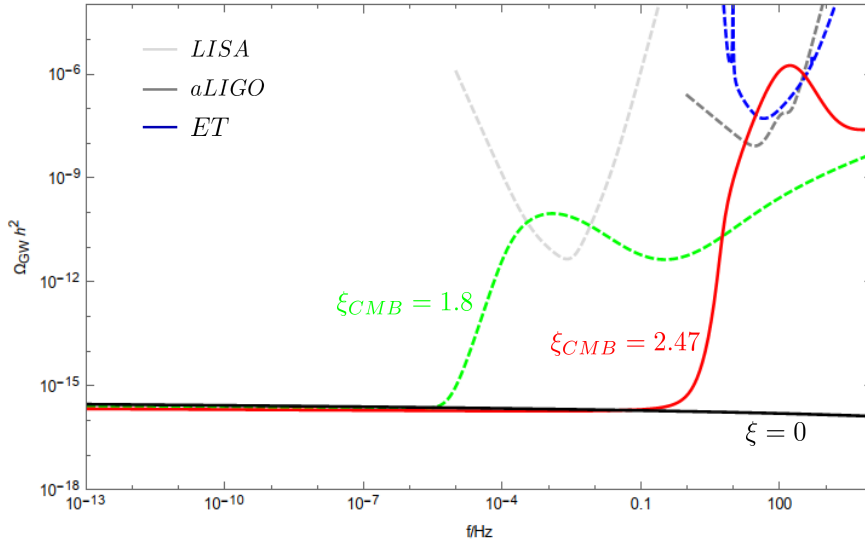


Figure 4.6: $\Omega_{\text{GW}} h^2$ as a function of the frequency f for $\xi_{\text{CMB}} = 0; 1.8; 2.47$. The latter was found for $\delta = 3$ and $\Delta = 0.2$, while for $\xi_{\text{CMB}} = 1.8$ $\delta = 0.7$ and $\Delta = 1$. We have required $N = 60$ e-foldings of observable inflation. For reference we also show the sensitivity curves of LISA, Advanced LIGO/VIRGO and Einstein Telescope.

acquires a bigger velocity for a steeper potential. For the same reason, the maximum is reached at earlier times, i.e. for smaller values of the frequency. Studying the shape of the hill as a function of δ is instead more complicated. The maximum value of Ω decreases if the steepness of the step gets smaller, as expected, given that the increase in velocity due to the step is smaller and consequently less gauge field and gravitational wave production takes place. However, the position of the peak does not display a monotonic behaviour, despite being directly related to the number of e-foldings necessary to the axion to reach first the top and then the bottom of the step in the potential.

This behaviour can be used to have a detectable signal also for advanced LIGO and ET. As can be seen from the red curve in figure 4.6, for the choice of parameters $\delta = 3$, $\Delta = 0.2$ and $\xi_{\text{CMB}} = 2.47$, and setting ϕ_0 to be at 15 e-foldings before the end of inflation, Ω_{GW} overlaps both sensitivity curves thanks to a very high peak. The description of the dynamics we provided before resembles the energy distribution in the Hubble and gauge field dissipative channels, as one can clearly see by inspecting the top-left panel of figure 4.7. However, despite the promising result one has to take into account also the backreaction effect on Friedmann equation. In the top-right panel of the same figure, we see as the presence of the peak in the density parameter is reflected in the relative energy of the gauge field, where a crest at $\simeq 0.1$ appears around 15 e-foldings before the end of

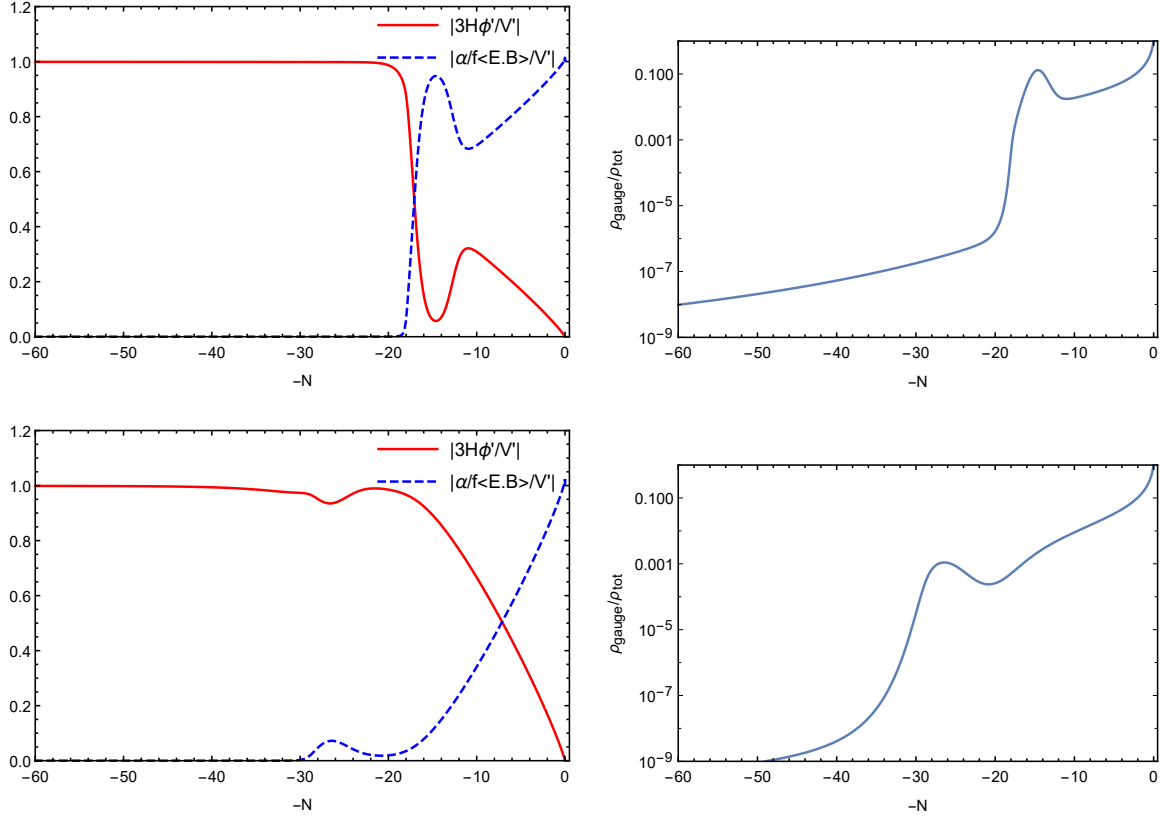


Figure 4.7: Friction terms in Klein-Gordon equation for ϕ (on the left panel) and relative strength of the energy density of the produced quanta (on the right panel) for $\xi_{CMB} = 2.47$ and $\xi_{CMB} = 1.8$, respectively on the top and on the bottom, for a potential of the form (4.27). For both values of ξ_{CMB} the contribution from the backreaction to Friedmann equation was neglected. See the main text for more details.

inflation, precisely when tensor modes are massively produced. It is therefore possible that beyond that point our assumptions, as well as our result for the waves signal, are not valid anymore.

Strong backreaction on Friedmann equation appears to be the main problem related to the possibility of detection of chiral gravitational waves within our ad-hoc designed potential, for both regimes of super- and sub-Planckian values of the width of the step Δ . A hill or a plateau formation in the relative energy of the gauge modes are mainly related to the strength of the coupling between the inflaton and the gauge field, i.e. on the values of ξ_{CMB} , and to the steepness of the potential in correspondence of the hyperbolic tangent modulation. Indeed, if ξ_{CMB} is small enough and the step is just a small correction of the linear potential, the production of tensor modes can be still enhanced at previous times with respect to axion monodromy models without leading to strong backreaction

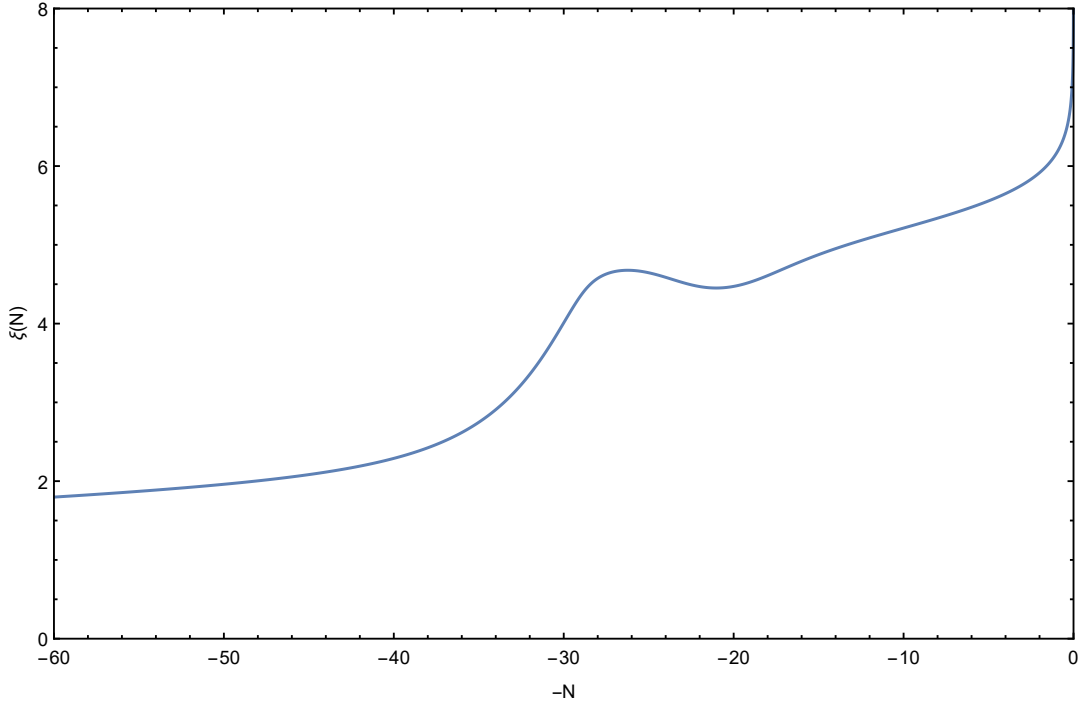


Figure 4.8: Evolution of ξ as a function of the number of efoldings. The small hill around 25 efoldings corresponds to the production of tensor modes when the inflaton is rolling down the step.

on Friedmann equation. The green curve of figure 4.6 represents an example. In this case we have set $\delta = 0.7$, $\Delta = 1$ and $\xi_{CMB} = 1.8$. A small hill allows for a superimposition between the signal of the tensor modes and LISA's sensitivity curve without spoiling our assumptions. Indeed, the backreaction on the inflaton becomes dominant only in the last $\simeq 10$ efoldings, as well as the relative energy contained in the gauge field, as shown in the bottom-left and bottom-right panel of figure 4.7, respectively. One last check needs to be done about whether or not for such small values of ξ_{CMB} the expressions for the tensor power spectrum in (4.14) and (4.15) still hold. By inspecting figure 4.8, one can see how $\xi \gtrsim 3$ before the production of tensor modes begins at approximately 30 efoldings before the end of inflation. Therefore, when step constitute only a small perturbation of the linear potential, a signal from chiral gravitational waves might be detected in future by LISA while respecting both the limit from nongaussianities and the weak backreaction on H assumption.

Chapter 5

Conclusions and outlook

To summarize, we have seen how the interaction between an axion-like inflaton and a gauge field can lead to a rich and complex phenomenology. As ϕ rolls down its potential, it provides a time-dependent background for the quantization of the gauge field, amplifying the vacuum fluctuations of one of its helicity modes into classical particles, which become a source of scalar and tensor perturbations. The gauge modes also backreact on the inflaton, slowing it down and providing a new dissipation channel in Klein-Gordon equation. As a result, the inflationary period is extended, leaving enough room to solve the Standard Cosmological model problems. The energy density in produced gauge field fluctuations contributes also to the Friedmann equation, but in our computations and numerical simulations we have systematically neglected it, while we kept its backreaction on the inflaton.

Since the gauge modes production is enhanced only at late times, these effects become important only towards the end of inflation and can hence be neglected at the CMB scales. Nevertheless, scalar perturbations arise also for such large scales due to the decay process $\delta A + \delta A \rightarrow \delta\phi$. Their power spectrum can be either red or blue, depending on the form of the inflaton potential. At smaller scales, at which interferometers work, we enter in a strong backreaction regime. Here is where gravitational waves are efficiently produced, and the parity-violating nature of the system is translated into a different power spectrum of the left-handed and right-handed modes. A net handedness of the tensor modes can then be checked if non-vanishing TE and TB correlation in the CMB are detected.

For natural inflation, the first axion-inflation model proposed, the interaction with the gauge field is essential to drive inflation, but in its simplest version the theory is unable to satisfy COBE normalization for the scalar power spectrum and to provide a detectable signal for chiral gravitational waves.

Similarly, whereas axion monodromy allows a scalar power spectrum in agreement with COBE normalization, the secondary tensor modes are still produced too late in the strong backreaction regime, and their frequency is therefore too large to be detected by

ongoing and future experiments.

We showed how a solution to this problem might come by considering a slightly different potential, where a linear behaviour is modified with the introduction of a suitable step. When the step is too steep or on the other hand too broad, the backreaction on the Friedmann equation becomes stronger and our results, even if promising, might need to be reviewed. Instead, if the step represents only a small correction to the well-studied linear potential, such large backreaction can be avoided and chiral gravitational waves might be detected in the future by LISA.

The work presented in this thesis has several possibilities for future extensions. It will be interesting to better understand the behaviour of our designed axion potential as a function of its parameters which describe the form and position of the step. Moreover, a more complete and more reliable study of the phenomenology of all three models can be made by taking into account also the backreaction of the gauge fluctuations on the evolution of Hubble parameter H . We leave these for future work.

Appendix A

Calculation of the scalar power spectrum

As discussed in chapter 3, the curvature perturbation power spectrum is related the two point function of the perturbations of the inflaton ϕ , whose expression is given in equation (3.28). In this appendix we find a solution for that expression and then derive the scalar power spectrum. In order to perform this calculation, we will first compute the two point correlator of $\delta_{\vec{E}\cdot\vec{B}}$ and the propagator $G(\tau, \tau')$.

A.1 Two-point function of $\delta_{\vec{E}\cdot\vec{B}}$

By using the definition in (3.26) and the properties discussed afterward, the correlator for $\delta_{\vec{E}\cdot\vec{B}}$ can be written as

$$\begin{aligned} \int d^3x e^{i\vec{p}\cdot\vec{x}} \langle 0 | \delta_{\vec{E}\cdot\vec{B}}(\tau', 0) \delta_{\vec{E}\cdot\vec{B}}(\tau'', \vec{x}) | 0 \rangle &= \frac{1}{a^4(\tau')a^4(\tau'')} \int \frac{d^3k}{(2\pi)^3} |\vec{k}| |\vec{\epsilon}_+(-\vec{k}) \cdot \vec{\epsilon}_+(\vec{p} + \vec{k})|^2 \times \\ &\times \left\{ |\vec{p} + \vec{k}| A'_+(\tau', -\vec{k}) A_+(\tau', \vec{p} + \vec{k}) A_+^*(\tau'', \vec{p} + \vec{k}) A_+^*(\tau'', -\vec{k}) + \right. \\ &\left. + |\vec{k}| A'_+(\tau', \vec{p} + \vec{k}) A_+(\tau', -\vec{k}) A_+^*(\tau'', \vec{p} + \vec{k}) A_+^*(\tau'', -\vec{k}) \right\}, \end{aligned} \quad (\text{A.1})$$

where we have also assumed that $A_-(\tau, \vec{k}) \simeq 0$. Since the generation of inhomogeneities in ϕ is enhanced for wavelengths larger than $(2\xi H)^{-1}$, where the electromagnetic field has large occupation numbers and can be treated as a classical source, there is no need to renormalize the expression above. In this regime we can use the approximation in 3.11

for $A_+(\tau, \vec{k})$, so that the correlator above becomes

$$\int d^3x e^{i\vec{p}\cdot\vec{x}} \langle 0 | \delta_{\vec{E}\cdot\vec{B}}(\tau', 0) \delta_{\vec{E}\cdot\vec{B}}(\tau'', \vec{x}) | 0 \rangle = \frac{e^{4\pi\xi}}{4a'^4 a''^4} \int \frac{d^3k}{(2\pi)^3} |\vec{\epsilon}_+(-\vec{k}) \cdot \vec{\epsilon}_+(\vec{p} + \vec{k})|^2 \times \\ \times e^{-4\sqrt{2\xi/\tilde{a}H}(\sqrt{|\vec{k}|} + \sqrt{|\vec{p} + \vec{k}|})} \{ |\vec{k}| |\vec{p} + \vec{k}| + |\vec{k}|^{3/2} |\vec{p} + \vec{k}|^{1/2} \}, \quad (\text{A.2})$$

where $\tilde{a}(\tau', \tau'')$ is defined vis $2/\sqrt{\tilde{a}} \equiv 1/\sqrt{a'} + 1/\sqrt{a''}$, with $a' \equiv a(\tau')$ and $a'' \equiv a(\tau'')$. Using the same reasoning we adopted after equation 3.12, we extend the integral from 0 to ∞ . After a change of integration variable, we finally write the correlator as

$$\int d^3x e^{i\vec{p}\cdot\vec{x}} \langle 0 | \delta_{\vec{E}\cdot\vec{B}}(\tau', 0) \delta_{\vec{E}\cdot\vec{B}}(\tau'', \vec{x}) | 0 \rangle = \quad (\text{A.3})$$

$$= e^{4\pi\xi} \frac{\tilde{a}^5}{a'^4 a''^4} \frac{H^5}{\xi^5} \mathcal{C} \left(\frac{2^5 \xi |\vec{p}|}{\tilde{a}H} \right), \quad (\text{A.4})$$

where the function $\mathcal{C}(\kappa)$, after directing \vec{p} along the z direction, reads

$$\mathcal{C}(\kappa) = \frac{\kappa^5}{2^{30} \pi^3} \int d^3q |\vec{\epsilon}_+(-\vec{q}) \cdot \vec{\epsilon}_+(\hat{z} + \vec{q})|^2 \times \quad (\text{A.5})$$

$$\times e^{-\sqrt{\kappa}(\sqrt{|\vec{q}|} - \sqrt{|\hat{z} + \vec{q}|})} |\vec{q}| |\hat{z} + \vec{q}| \left\{ 1 + \frac{|\vec{q}|^{1/2}}{|\hat{z} + \vec{q}|^{1/2}} \right\}, \quad (\text{A.6})$$

where \hat{z} is the versor of the z axis.

A.2 The Green function

Although the Green function for equation (3.24) can be computed exactly, we will limit ourselves to the case of the cosine potential $V(\Phi) \propto 1 + \cos(\Phi/f)$, which allows us to obtain a simpler analytical expression. In this case, $V'(\Phi_0) \sim V(\Phi_0)/f$, $V''(\Phi_0) \sim V(\Phi_0)/f^2$, $H^2 \sim V(\Phi_0)/M_P^2$ and $\alpha \gg 1$ while $f \lesssim M_P$. This allows to see that the coefficient of $d\phi/d\tau$ in equation (3.24) is much larger than one. Moreover, we can neglect the term p^2 in the coefficient of ϕ since $|p| \ll a\sqrt{|V''|} \simeq (M_P/f)aH$, which is always true for $p \ll 2\xi aH$. Once we have taken into account these two approximations, the Green function can be obtained by solving

$$\frac{\partial^2 G(\tau, \tau')}{\partial \tau^2} - \frac{1}{\tau} \frac{\pi \alpha V'(\Phi_0)}{f H^2} \frac{\partial G(\tau, \tau')}{\partial \tau} + \quad (\text{A.7})$$

$$+ \frac{V''(\Phi_0)}{H^2 \tau^2} G(\tau, \tau') = \delta(\tau - \tau'), \quad (\text{A.8})$$

with $G(\tau', \tau') = 0$ and $(\partial G/\partial \tau)(\tau', \tau') = 1$, whose solution is

$$G(\tau, \tau') = \begin{cases} \frac{\tau'}{\nu_+ - \nu_-} \left[\left(\frac{\tau}{\tau'} \right)^{\nu_+} - \left(\frac{\tau}{\tau'} \right)^{\nu_-} \right], & \tau > \tau' \\ 0, & \tau < \tau' \end{cases}$$

where

$$\nu_{\pm} \simeq \frac{\pi \alpha V'(\Phi_0)}{2fH^2} \left[1 \pm \sqrt{1 - \frac{4}{\pi^2} \frac{1}{\alpha^2} \frac{V''(\Phi_0)H^2 f^2}{V'(\Phi_0)^2}} \right]. \quad (\text{A.9})$$

The second term under the square root in equation (A.9) scales as $(f/\alpha M_P)^2$ and is much smaller than one. Therefore, we have $\nu_+ \simeq \pi \alpha V'/(fH^2) \propto \alpha M_P^2/f^2 \gg 1$ whereas $\nu_- \simeq V''f/(\pi \alpha V') \propto 1/\alpha \ll 1$.

A.3 The scalar power spectrum

As we are interested in the spectrum at $p \ll aH$, we can neglect the term $(\tau/\tau')^{\nu_+}$ in the expression of the Green function, that goes rapidly to zero. Using the previous results, $a = -1/H\tau$ and changing the integration variables $w' = -(2^5 \xi |\vec{p}| \tau')^{-1}$, $w'' = -(2^5 \xi |\vec{p}'| \tau'')^{-1}$, the two-point function reads

$$\langle \phi(\vec{p}) \phi(\vec{p}') \rangle = \frac{\delta^3(\vec{p} + \vec{p}')}{p^3} \frac{\mathcal{N} \alpha H^4 e^{4\pi\xi}}{\nu_+^2 f^2 \xi^8} \frac{e^{4\pi\xi}}{2^{15}} \left(\frac{2^5 \xi p}{aH} \right)^{2\nu_-} \quad (\text{A.10})$$

$$\times \int_0^{\frac{aH}{2^5 \xi p}} dw' w'^{\nu_- - 5} \int_0^{\frac{aH}{2^5 \xi p'}} dw'' w''^{\nu_- - 5} \tilde{w}^5 \mathcal{C}(\tilde{w}^{-1}), \quad (\text{A.11})$$

where we have defined $2/\sqrt{\tilde{w}} \equiv 1/\sqrt{w'} + 1/\sqrt{w''}$. We see that, as long as $\nu_- \ll 1$ the spectrum of perturbations in the inflaton is quasi-scale invariant. To find the normalization, we send $p \rightarrow 0$ in the limits of integration.

The integral can then be computed by performing another change of variables $x' = w'^{-1/4}$, $x'' = w''^{-1/4}$ and going to "polar coordinates" $x' = \rho \cos(\theta)$, $x'' = \rho \sin(\theta)$. To simplify the resulting expression we set $\nu_- = 0$. Using the expression A.6 for the function \mathcal{C} , the integrals in θ and ρ can now be computed explicitly:

$$\int_0^\infty \frac{dw'}{w'^5} \int_0^\infty \frac{dw''}{w''^5} \tilde{w}^5 \mathcal{C}(\tilde{w}^{-1}) = \frac{\Gamma(8)\Gamma(6)}{2^{27} \pi^{5/2} \Gamma(\frac{17}{2})} \times \quad (\text{A.12})$$

$$\times \int d^3 q |\vec{\epsilon}_+(-\vec{q}) \cdot \vec{\epsilon}_+(\hat{z} + \vec{q})|^2 \frac{|\vec{q}| |\hat{z} + \vec{q}| + |\vec{q}|^{3/2} |\hat{z} + \vec{q}|^{1/2}}{\left(\sqrt{|\vec{q}|} + \sqrt{|\hat{z} + \vec{q}|} \right)^{16}} \quad (\text{A.13})$$

, where the integral in $d^3 q$ can be evaluated numerically to $\simeq 3.5 \times 10^{-4}$. We have now all the ingredients to find the two-point function of the scalar perturbations, which can

be written as follows:

$$\langle \phi(\vec{p})\phi(\vec{p}') \rangle = \gamma \frac{\delta^3(\vec{p} + \vec{p}')}{p^3} \frac{\mathcal{N}\alpha^2}{\nu_+^2 f^2} e^{4\pi\xi} \frac{H^4}{\xi^8} \left(\frac{2^5 \xi p}{aH} \right)^{2\nu_-}, \quad (\text{A.14})$$

where the numerical factor has value $\gamma \simeq 2.1 \times 10^{-6}$. From the formula above we can extract the curvature perturbation $\mathcal{P}_\zeta = p^3 H^2 \langle \phi\phi \rangle / [2\pi^2 \dot{\Phi}_0^2 \delta^3(\vec{p} + \vec{p}')]$, which, after using $\alpha(H/\xi)^4 e^{2\pi\xi} = fV'/\mathcal{I}$, has the form

$$\mathcal{P}_\zeta = \frac{\gamma}{8\pi^4 \mathcal{I}^2} \frac{1}{\xi^2} \left(\frac{2^5 \xi p}{aH} \right)^{2\nu_-} \simeq \frac{5 \times 10^{-2}}{\xi^2} \left(\frac{2^5 \xi p}{aH} \right)^{2\nu_-}. \quad (\text{A.15})$$

If the theory contains \mathcal{N} gauge fields, the different contributions to the two-point function of $\delta_{\vec{E}, \vec{B}}$ adds incoherently, leading to a suppression by a factor of \mathcal{N} of \mathcal{P}_ζ , i.e.

$$\mathcal{P}_\zeta \simeq \frac{5 \times 10^{-2}}{\mathcal{N} \xi^2} \left(\frac{2^5 \xi p}{aH} \right)^{2\nu_-}. \quad (\text{A.16})$$

Appendix B

Calculation of the tensor power spectrum

The starting point for computing the tensor power spectrum is the equation of motion for the tensor perturbations $h_{ij}(\tau, \vec{x})$ given in (4.4), which we rewrite here for simplicity:

$$h''_{ij} + 2\frac{a'}{a}h'_{ij} - \Delta h_{ij} = \frac{2}{M_P^2}\Pi_{ij}{}^{lm}T_{lm}^{\text{EM}}. \quad (\text{B.1})$$

Moving to momentum space and projecting h_{ij} into positive and negative helicity modes, we have

$$h^{ij}(\vec{k}) = \sqrt{2} \sum_{\lambda=\pm} \epsilon_{\lambda}^i(\vec{k})\epsilon_{\lambda}^j(\vec{k})h_{\lambda}(\tau, \vec{k}), \quad (\text{B.2})$$

where the amplitude $h_{\lambda}(\vec{k})$ is given by the relation $\Pi_{\pm}^{ij}(\vec{k}) = \epsilon_{\mp}^i(\vec{k})\epsilon_{\mp}^j(\vec{k})/\sqrt{2}$ and the helicity vectors satisfy the properties $k_i\epsilon_{\pm}^i = 0$, $\varepsilon_{abc}k^b\epsilon_{\pm}^c = \mp ik\epsilon_{\pm}^c$, $\epsilon_{\pm}^i\epsilon_{\mp}^i = 1$ and $\epsilon_{\pm}^i\epsilon_{\pm}^i = 0$. We can now promote the functions h_{\pm} to operators.

The Green function associated to the homogeneous part of (B.1) can be easily calculated and has the form, for $\tau > \tau'$,

$$G_k(\tau, \tau') = \frac{1}{k^3\tau'^2}[(1 + k^2\tau\tau')\sin[k(\tau - \tau')] + k(\tau' - \tau)\cos[k(\tau - \tau')]], \quad (\text{B.3})$$

while $G_k(\tau < \tau') = 0$. Hence, the expression for $\hat{h}_{\pm}(\vec{k})$ is given by the formula

$$\hat{h}_{\pm}(\vec{k}) = -\frac{2H^2}{M_P^2} \int d\tau' G_k(\tau, \tau')\tau'^2 \int \frac{d^3q}{(2\pi)^{3/2}} \Pi_{\pm}^{lm}(\vec{k}) \times \quad (\text{B.4})$$

$$\times \left[\hat{A}'_i(\vec{q}, \tau')\hat{A}'_m(k - \vec{q}, \tau') - \varepsilon_{lab}q_a\hat{A}'_b(\vec{q}, \tau')\varepsilon_{mcd}(k_c - q_c)\hat{A}'_m(k - \vec{q}, \tau') \right], \quad (\text{B.5})$$

where we have written in the traceless and transverse part of the energy-momentum tensor $T_{ij}^{\text{EM}} = -a^2(E_iE_j + B_iB_j)$ the electric and magnetic fields in terms of the four-potential $A(\tau, \vec{k})$.

Since the production of tensor modes is efficient only for $(8\xi)^{-1} \ll |k\tau| \ll 2\xi$, we use the approximated form in equation (3.11) for A_+ , while we set $A_- = 0$. The two-point function for a gravitational wave with general helicity λ can be computed using Wick's theorem:

$$\begin{aligned} \langle 0 | h_\lambda(\vec{k}) h_\lambda(\vec{k}') | 0 \rangle &= \frac{4H^4}{M_P^4} \int d\tau' d\tau'' (\tau')^2 (\tau'')^2 G_k(\tau, \tau') G_{k'}(\tau, \tau'') \times \\ &\int \frac{d^3q}{(2\pi)^3} \langle 0 | \left\{ \Pi_\lambda^{ij*}(\vec{k}) \times \left[\hat{A}_i^*(\vec{q}, \tau') \hat{A}_j^*(\vec{k} - \vec{q}, \tau') - \varepsilon_{iab} q_a \hat{A}_b^*(\vec{q}, \tau') \varepsilon_{jcd} (k_c - q_c) \hat{A}_d^*(\vec{k} - \vec{q}, \tau') \right] \right\} \\ &\left\{ \Pi_\lambda^{ij}(\vec{k}') \times \left[\hat{A}_i(\vec{q}, \tau'') \hat{A}_j(\vec{k}' - \vec{q}, \tau'') - \varepsilon_{irs} q_r \hat{A}_s(\vec{q}, \tau'') \varepsilon_{jtv} (k_t - q_t) \hat{A}_v(\vec{k}' - \vec{q}, \tau'') \right] \right\} | 0 \rangle. \end{aligned} \quad (\text{B.6})$$

This equation can be computed using the decomposition into creation and annihilation operators for the four-potential

$$\hat{A}_i(\tau, \vec{k}) = \sum_{\lambda=\pm} \left[\epsilon_\lambda^i(\vec{k}) A_\lambda(\tau, \vec{k}) \hat{a}_\lambda^{\vec{k}} e^{i\vec{k}\cdot\vec{x}} + h.c. \right] = \epsilon_+^i(\vec{k}) A_+(\tau, \vec{k}) \hat{a}_\vec{k}^+ e^{i\vec{k}\cdot\vec{x}} + h.c., \quad (\text{B.7})$$

where $\hat{a}_\vec{k}^+$ and $\hat{a}_{-\vec{k}}^{+\dagger}$ satisfy the standard commutation relations

$$\left[\hat{a}_\vec{k}^+, \hat{a}_{\vec{k}'}^{+\dagger} \right] = \delta^3(\vec{k} - \vec{k}') \quad (\text{B.8})$$

$$\left[\hat{a}_\vec{k}^+, \hat{a}_{\vec{k}'}^+ \right] = \left[\hat{a}_\vec{k}^{+\dagger}, \hat{a}_{\vec{k}'}^{+\dagger} \right] = 0. \quad (\text{B.9})$$

In equation (B.6) there are four products, but only the first one involving only time derivatives of \hat{A} gives a non-vanishing result. Indeed, by inspecting the other three terms one can see that they contains combinations of the helicity vectors of the form

$$\epsilon_{-\lambda}^i(\vec{k}) \epsilon_{-\lambda}^j(\vec{k}) \epsilon_{-\lambda}^i(\vec{q}) \epsilon_{-\lambda}^j(\vec{k} - \vec{q}) \epsilon_{-\lambda}^i(\vec{k}) \epsilon_{-\lambda}^j(\vec{k}) \varepsilon_{irs} q_r \epsilon_+^s(\vec{q}) \varepsilon_{jtv} (k_t - q_t) \epsilon_+^v(\vec{k} - \vec{q}), \quad (\text{B.10})$$

$$\epsilon_{-\lambda}^i(\vec{k}) \epsilon_{-\lambda}^j(\vec{k}) \varepsilon_{iab} q_a \epsilon_-^b(\vec{q}) \varepsilon_{jcd} (k_c - q_c) \epsilon_-^d(\vec{k} - \vec{q}) \epsilon_{-\lambda}^i(\vec{k}) \epsilon_{-\lambda}^j(\vec{k}) \varepsilon_{irs} q_r \epsilon_+^s(\vec{q}) \varepsilon_{jtv} (k_t - q_t) \epsilon_+^v(\vec{k} - \vec{q}) \quad (\text{B.11})$$

which vanish due to the properties $\varepsilon_{abc} k^b \epsilon_\pm^c = \mp i k \epsilon_\pm^c$, $\epsilon_\pm^i \epsilon_\pm^i = 0$ and $\epsilon_\pm^i \epsilon_\mp^i = 1$. Therefore, from now on we will focus only on the first term, which we write explicitly:

$$\begin{aligned} \langle 0 | h_\lambda(\vec{k}) h_\lambda(\vec{k}') | 0 \rangle &= \frac{4H^4}{M_P^4} \int d\tau' d\tau'' (\tau')^2 (\tau'')^2 G_k(\tau, \tau') G_{k'}(\tau, \tau'') \times \\ &\int \frac{d^3q}{(2\pi)^3} \langle 0 | \left[\Pi_\lambda^{ij*}(\vec{k}) \hat{A}_i^*(\vec{q}, \tau') \hat{A}_j^*(\vec{k} - \vec{q}, \tau') \right] \times \left[\Pi_\lambda^{ij}(\vec{k}') \hat{A}_i(\vec{q}, \tau'') \hat{A}_j(\vec{k}' - \vec{q}, \tau'') \right] | 0 \rangle \end{aligned} \quad (\text{B.12})$$

Looking the decomposition in (B.7), we see there are 16 different products of creation and annihilation operators acting on the vacuum in the equation above. Among them, 12 are trivially zero and 3 between the remaining combinations are zero after using the commutation relations. The only combination which gives a contribution is

$$\langle 0 | \hat{a}_{\vec{q}}^+ \hat{a}_{\vec{k}-\vec{q}}^+ \hat{a}_{-\vec{q}}^{+\dagger} \hat{a}_{-\vec{k}'+\vec{q}}^{+\dagger} | 0 \rangle. \quad (\text{B.13})$$

Hence, the final result for the two-point function of the tensor perturbations is, using again (B.7),

$$\langle h_\lambda(\vec{k}) h_\lambda(\vec{k}') \rangle = \frac{H^4 \xi}{4\pi^3 M_P^4} e^{4\pi\xi} \delta(\vec{k} + \vec{k}') \int d\tau' d\tau'' |\tau'|^{3/2} |\tau''|^{3/2} G_k(\tau, \tau') G_k(\tau, \tau'') \times \quad (\text{B.14})$$

$$\times \int d^3\vec{q} |\epsilon_{-\lambda}^i(\vec{k}) \epsilon_+^i(\vec{q})|^2 |\epsilon_{-\lambda}^j(\vec{k}) \epsilon_+^j(\vec{k}-\vec{q})|^2 \sqrt{|\vec{k}-\vec{q}|} \sqrt{q} e^{-2\sqrt{2}\xi(\sqrt{|\tau'|} + \sqrt{|\tau''|})(\sqrt{q} + \sqrt{|\vec{k}-\vec{q}|})}. \quad (\text{B.15})$$

Bibliography

- [1] D. S. Gorbunov and V. A. Rubakov, *Introduction to the Theory of the Early Universe: Cosmological Perturbations and Inflationary Theory*, World Scientific Publishing, 2011.
- [2] D. Mukhanov, *Physical Foundations of Cosmology*, Cambridge University Press, 2019.
- [3] R. d’Inverno, *Introducing Einstein Relativity*, Clarendon Press, Oxford, 1992.
- [4] S. Weinberg, *Gravitation and Cosmology: Principles and Applications of the General Theory of Relativity*, John Wiley and Sons, 1972.
- [5] M. Srednicki, *Quantum Field Theory*, Cambridge University Press, 2007.
- [6] P.C.W. Davies N. D. Birrell, *Quantum Fields in Curved Space*, Cambridge University Press, 1982.
- [7] M. Maggiore, *Gravitational Waves, volume 2: Astrophysics and Cosmology*, Oxford University Press, 2018.
- [8] A. Riotto, *Inflation and the Theory of Cosmological Perturbations*, arXiv:hep-ph/0210162v2, 2017.
- [9] M. M. Anber and L. Sorbo, *Naturally inflating on steep potentials through electromagnetic dissipation*, arXiv:0908.4089 [hep-th], 2010.
- [10] L. Sorbo, *Parity violation in the Cosmic Microwave Background from a pseudoscalar inflaton*, arXiv:1101.1525 [astro-ph.CO], 2011.
- [11] M. M. Anber and L. Sorbo, *Non-Gaussianities and chiral gravitational waves in natural steep inflation*, arXiv:1203.5849v1 [astro-ph.CO], 2012.
- [12] N. Barnaby and M. Peloso, *Large Nongaussianity in Axion Inflation*, arXiv:1011.1500 [hep-ph], 2010.
- [13] N. Barnaby, R. Namba and M. Peloso, *Phenomenology of a Pseudo-Scalar Inflaton: Naturally Large Nongaussianity*, arXiv:1102.4333 [astro-ph.CO], 2011.

- [14] N. Barnaby, E. Pajer and M. Peloso, *Gauge Field Production in Axion Inflation: Consequences for Monodromy, non-Gaussianity in the CMB, and Gravitational Waves at Interferometers*, arXiv:1110.3327v1 [astro-ph.CO], 2011.
- [15] L. A. Boyle and P. J. Steinhardt, *Probing the early universe with inflationary gravitational waves*, arXiv:astro-ph/0512014, 2005.
- [16] V. Domcke, V. Guidetti, Y. Welling and A. Westphal, *Resonant backreaction in axion inflation*, arXiv:2002.02952v2 [astro-ph.CO], 2020.
- [17] R. Namba, M. Peloso, M. Shiraishi, L. Sorbo and C. Unal, *Scale-dependent gravitational waves from a rolling axion*, arXiv:1509.07521v1 [astro-ph.CO], 2015.
- [18] N. Aggarwal, O.D. Aguiar *et al.*, *Challenges and Opportunities of Gravitational Wave Searches at MHz to GHz Frequencies*, arXiv:2011.12414v1 [gr-qc], 2020.
- [19] N. Bartolo, C. Caprini, V. Domcke *et al.*, *Science with the space-based interferometer LISA. IV: probing inflation with gravitational waves*, arXiv:1610.06481v2 [astro-ph.CO], 2016.
- [20] T. Robson, N. J. Cornish and C. Liu, *The construction and use of LISA sensitivity curves*, arXiv:1803.01944v2 [astro-ph.H], 2018.
- [21] L. Barsotti, P. Fritschel *et al.*, *Updated Advanced LIGO sensitivity design curve*, <https://dcc.ligo.org/LIGO-T1800044/public>.
- [22] B. F. Schutz and B. S. Sathyaprakash, *Physics, Astrophysics and Cosmology with Gravitational Waves*, arXiv:0903.0338v1, 2009.
- [23] C. J. Moore, R. H. Cole, C. P. L. Berry *Gravitational-wave sensitivity curves*, arXiv:1408.0740v2 [gr-qc], 2014.
- [24] Planck Collaboration, *Planck 2018 results. VI. Cosmological parameters*, arXiv:1807.06209v4 [astro-ph.CO], 2021.
- [25] Planck Collaboration, *Planck 2018 results. IX. Constraints on primordial non-Gaussianity*, arXiv:1905.05697 [astro-ph.CO], 2019.
- [26] Planck Collaboration, *Planck 2018 results. X. Constraints on inflation*, arXiv:1807.06211v2 [astro-ph.CO], 2019.
- [27] J. Adams, B. Cresswell and R. Easther, *Inflationary perturbations from a potential with a step*, arXiv:astro-ph/0102236, 2001.
- [28] L. McAllister, E. Silverstein and A. Westphal *Gravity Waves and Linear Inflation from Axion Monodromy*, arXiv:0808.0706, 2010.